ACS OMEGA

Open Access

http://pubs.acs.org/journal/acsodf

Article

Deciphering the Immunogenicity of Monkeypox Proteins for Designing the Potential mRNA Vaccine

Mohibullah Shah,* Samavia Jaan, Muhammad Shehroz, Asifa Sarfraz, Khamna Asad, Tehreem Ul Wara, Aqal Zaman, Riaz Ullah, Essam A. Ali, Umar Nishan, and Suvash Chandra Ojha*

Cite This: *ACS Omega* 2023, 8, 43341−43355

Read Online

ACCESS | Metrics & More | Article Recommendations | Supporting Information

ABSTRACT: The Monkeypox virus (MPXV), an orthopox virus, is responsible for monkeypox in humans, a zoonotic disease similar to smallpox. This infection first appeared in the 1970s in humans and then in 2003, after which it kept on spreading all around the world. To date, various antivirals have been used to cure this disease, but now, MPXV has developed resistance against these, thus increasing the need for an alternative cure for this deadly disease. In this study, we devised a reverse vaccinology approach against MPXV using a messenger RNA (mRNA) vaccine by pinning down the antigenic proteins of this virus. By using bioinformatic tools, we predicted prospective immunogenic B and T lymphocyte epitopes. Based on cytokine inducibility score, nonallergenicity, nontoxicity, antigenicity, and conservancy, the final epitopes were selected. Our analysis revealed the stable structure of the mRNA vaccine and its efficient expression in host cells. Furthermore, strong interactions were demonstrated with toll-like receptors 2 (TLR2) and 4 (TLR4) according to the molecular dynamic simulation studies. The in silico immune simulation analyses revealed an overall increase in the immune responses following repeated exposure to the designed vaccine. Based on our findings, the vaccine candidate designed in this study has the potential to be tested as a promising novel mRNA therapeutic vaccine against MPXV infection.

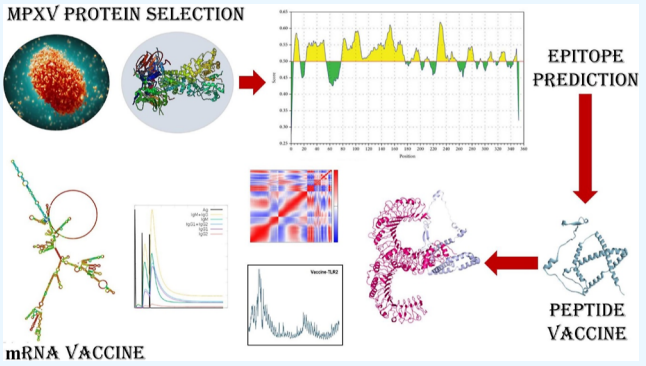

1. INTRODUCTION

Monkeypox, caused by an orthopox virus, i.e., the monkeypox virus (MPXV) is a disease that was recognized in nonhuman hosts before the 1970s.[1] MPXV is a linear, enveloped dsDNA virus that belongs to the *Poxviridae* family with a size ranging from 200 to 250 nm. The size of the MPXV genome is approximately 197kb, which contains ∼190 overlapping open reading frames (ORFs).[2] The central coding region sequence in MPXV, like all the orthopox viruses at nucleotide positions 56,000−120,000, is a highly conserved sequence that is flanked by variable ends consisting of inverted terminal repeats (ITRs).[3] The genes found in the terminal sites of the MPXV genome are homologous to those in the Vaccinia virus (VACV). These homologues play a major role in immunomodulation and are either known or predicted to influence pathogenicity and host range determination.[3] In the ITR region, MPXV, unlike the Variola virus with no ORFs, consists of at least 4 ORFs.[4]

MPXV is transmitted by two means: animals−human and human−human transmissions.[5] Direct contact with the blood, body fluids, and mucosal or cutaneous lesions of infected animals can result in animal-to-human (zoonotic) transfer.[6] Recently contaminated objects, sore skin of an infected individual, and close contact with respiratory secretions can result in human-to-human transmission.[7] The first outbreak of MPXV was documented in monkeys in 1959 in Denmark.[8] In the Democratic Republic of the Congo, a nine-month-old infant was found to have the first human incidence of MPXV. From October 1970 to May 1971, six MPXV cases in humans were reported in Liberia, Sierra Leone, and Nigeria.[9] Since then, thousands of human cases of monkeypox have been documented in 15 locations, with 11 of those locations being in Africa. The first outbreak of MPXV that was documented outside of Africa occurred in the USA in 2003 and was attributed to contact with MPXV-infected pet prairie dogs.[10] After that, more than 70 cases of MPXV were reported due to this outbreak in the USA. From 2018 onward, the monkeypox cases have also been documented in travelers from Nigeria to Israel, the UK, Singapore, and last, a number of nonendemic nations.[11] According to the W.H.O. report, 10 nations were reported with the greatest overall MPXV cases worldwide,

Received: October 9, 2023
Revised: October 17, 2023
Accepted: October 18, 2023
Published: October 30, 2023

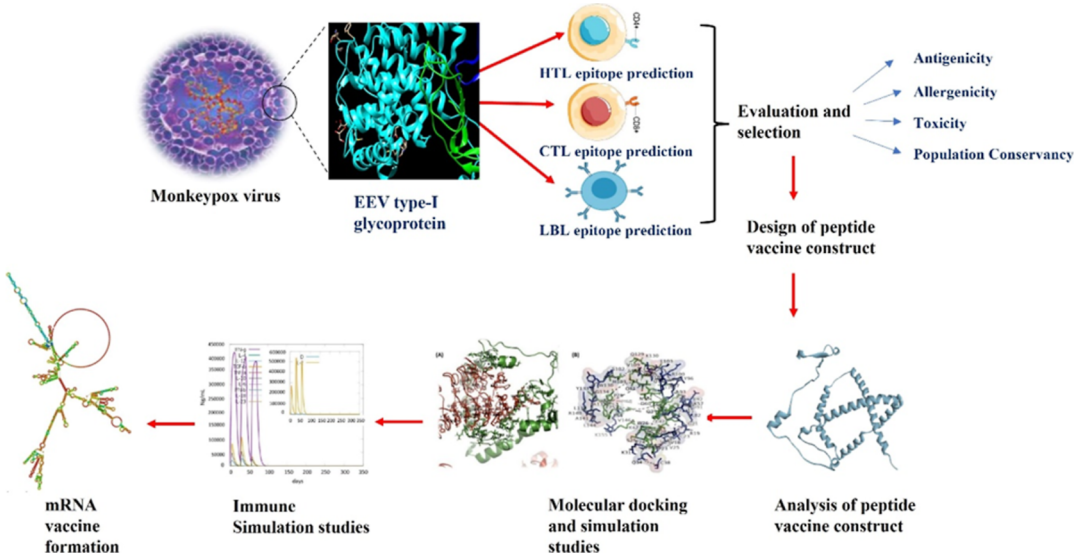

Figure 1. Workflow of the in silico MPXV vaccine design process.

including Canada (n = 1478), Germany (n = 3692), the UK (n = 3738), Peru (n = 3785), Mexico (n = 3937), Colombia (n = 4089), France (n = 4128), Spain (n = 7546), Brazil (n = 10,890), and the USA (n = 30,063). Collectively, 84.6% of all reported cases worldwide originate from these ten nations.[12]

Monkeypox symptoms are strikingly similar to smallpox symptoms. After infection, there is an incubation phase of around 10−14 days, followed by a prodrome period (a period before a rash develops) of 2 days. An infected person may experience symptoms like headache, fever, chills, malaise, swollen lymph nodes, backache, sore throat, and shortness of breath in the inguinal, cervical, or submandibular areas.[13] There have been several antiviral drugs such as Tecovirimat, Cidofovir, and Brincidofovir developed so far that have been approved by the FDA against different diseases and have shown effective results against orthopox viruses including monkeypox.[14−16] The Disease Control and Prevention (CDC) report states that although the human medical trials of Tecovirimat were found to be acceptable and safe, not enough information is available regarding its efficiency in treating orthopox viruses in humans. Cidofovir and brincidofovir proved to be effective against orthopox viruses both in vitro and in animal models.[14,15]

Studies have demonstrated that smallpox vaccination offers cross-protection against MPXV. It was found that people who received the smallpox vaccine had an 85% protection rate against MPXV. The CDC-recommended smallpox vaccination (ACAM2000TM) was found to reduce symptoms but not prevent the illness. The FDA and the EMA have also granted approval for IMVAMUNE, an attenuated third-generation MVA vaccine, to prevent monkeypox in adults. ACAM2000 and IMVAMUNE have neither been authorized for use in the general populace as of yet due to their unclear effects on immunosuppressed individuals and the reliability of vaccines that contain live VACV.[6,17]

The only FDA-approved vaccine against MPXV is JYNNEOS. It is a live, nonreplicating weakened Orthopox or the modified Vaccinia Ankara-Bavarian Nordic virus vaccine.[18] However, the JYNNEOS vaccine administration results in several side effects in the individuals, such as induration, chills, headache, sore throat, nausea, redness, myalgia, firmness/tightening, and pain.[18] In a population cohort in the Northwestern United States (Oregon), Sharff et al. conducted a retrospective study and found 10 occurrences of cardiac events following the administration of the JYNNEOS vaccine between July and October 2022.[19] Therefore, there is a need for a vaccine which could treat MPXV with no side effects.

Different studies have identified the RNA vaccination as a more productive and successful therapeutic option than the alternative in order to prevent these negative scenarios.[20,21] In order to be effective, messenger RNA (mRNA)-based therapies do not require the passage of the nuclear membrane, in contrast to DNA vaccines, which pose the risk of insertion of the viral genome into the genome of the host, which could lead to mutation.[21] Furthermore, mRNA vaccines can express the target proteins more effectively due to their expression in the cytoplasm as compared to the DNA-based vaccines, which require a nucleus for their expression.[22] The risk of incorporation into the genetic material is reduced by the RNA vaccines' targeting of the cytoplasm. Major histocompatibility complex (MHC) haplotype restriction is not present in mRNA vaccines, in contrast to epitope- based immunizations. Therefore, the mRNA vaccines can generate a quick immune response as compared with the epitope-based vaccines. Although the mRNA vaccines are themselves very effective, adding an adjuvant can further boost their immunogenicity. Furthermore, pattern recognition receptors were utilized to identify mRNA.[23] In clinical trials, this mRNA vaccine has demonstrated superior performance against a variety of infectious diseases and malignancies due to its high efficacy, few side effects, and affordable production costs.[24−26]

In MPXV-infected cells, two main forms of infectious virions are the extracellular enveloped virus (EEV) and the intracellular mature virus (IMV). Within the infected host, rapid long-distance spread of the virus is due to EEV, which is secreted from cells through interaction with the actin tail, as compared to IMV, which is released via cell lysis.[27] Thus, EEV is taken as the target protein to be used as a therapeutic and prophylactic cure against MPXV. To develop an mRNA vaccine construct, we used computational approaches to analyze the MPXV-encased glycoprotein. To create a peptide vaccine construct, we divulged the most antigenic and

https://doi.org/10.1021/acsomega.3c07866
ACS Omega 2023, 8, 43341−43355

immunogenic B- and T-cell epitopes and back-translated them. In order to increase the translation efficiency, we also adjusted the codons in the conserved mRNA construct. Along with docking approaches and immunological simulation techniques, we also sought to identify the 3D structure of the peptide vaccine construct using a variety of bioinformatics tools. The fundamental objective of this study is to support future laboratory attempts to create potent vaccines to prevent MPXV infections.

2. MATERIALS AND METHODS

Figure 1 depicts the pipeline for the mRNA vaccine against MPXV infection.

2.1. Retrieval of Envelope Glycoprotein and Consensus Sequence Identification. Reliable data are necessary for the production of an effective vaccine, so a literature survey was conducted to identify the best vaccine candidates that could be effective against MPXV infection. The NCBI database was used to find every accessible sequence of selected EEV glycoproteins, EEV Type-I membrane glycoprotein, and envelope protein H3. Using the Bioedit program included with Clustal W, all of the obtained protein sequences were aligned via multiple sequence alignment (MSA).[28] A consensus sequence was created using Bioedit's built-in tool after getting the aligned sequences. These consensus sequences were analyzed for various parameters, including physiochemical properties and antigenicity of proteins, for the final vaccine candidate selection.

2.2. Prediction of T-Cell Epitopes. Two T-lymphocyte types, i.e., helper T-cells (HTLs) and cytotoxic T-cells (CTLs), have the capacity to bind to MHC molecules and initiate cell-mediated immune responses. IEDB-Analysis Resource's NetMHCpanEL 4.1 technique was utilized to determine the epitopes of CTLs.[29] On the basis of the reference, the set of MHC-I alleles with a conservancy of >97% and a "9-mer" peptide length was chosen.[30] The leftover epitopes were selected on the basis of <0.2 threshold because they displayed maximum binding affinity with the MHC-I molecules. The IEDB-AR database was used to determine HTL epitopes. The parameters chosen were a referral set of alleles of MHC-II having >99% population conservancy and demonstrating a predicted epitope length of "15 mer". The epitopes were filtered based on a rank of <2.0 or lower for MHC−II binding epitopes. The projected epitope's capacity to engage with MHC molecules increases with decreasing rank.[31,32]

2.3. T-Cell-Predicted Epitope Analysis. Various criteria were examined in order to choose the most promising T-cell epitopes. The servers Vaxijen v2.0[33] and Allergenfp[34] were used to calculate the allergenicity and antigenicity, respectively. The Toxinpred server[35] was used to forecast harmful reactions. The conservation of amino acids in predicted epitopes was calculated by using IEDB's conservation analysis tool. The examination of various T-cell epitopes required that certain additional parameters be established. For T-cell epitopes that interact with MHC-I (CTL epitopes), we utilized the IEDB database's Class-I immunogenicity server. Similar to this, T-cells that interact with MHC-II (HTL epitopes) were also tested by the IFN-epitope, IL4-pred, and IL10-pred servers for their capacity to induce IFN gamma, IL-4, and IL-10.[36−38] Final T-cell epitope selections were made in order to build a vaccine against pathogen infection.

2.4. Prediction and Analysis of B-Cell Epitopes. The pathogen protein sequences represented by the LBL epitopes can attach to B lymphocytes and trigger an immune reaction. It was ascertained by utilizing the online BCEPRED server for predicting B-cell epitopes.[39] For the preference of high-affinity epitopes, a threshold of 75% specificity was chosen. Different servers were utilized to estimate the antigenicity (Vaxijenv2.0), allergenicity (Allergenfp), and toxicity (Toxinpred) of B-cell epitopes.[40] Conservancy analysis was also performed for predicted epitopes by employing the IEDB's conservancy analysis tool.

2.5. Population Coverage Analysis of the Selected T-Cell Epitopes. The population coverage analysis of the T-cell epitopes along with their corresponding alleles was performed by using the Population Coverage tool present within the IEDB database (http://tools.iedb.org/population/)[41] to ensure that the epitopes selected for the vaccine formulation would cover the majority of the world's population. This tool is used to calculate the average coverage of epitopes in various populations on the basis of the distribution of their MHC-binding alleles. The worldwide analysis of the epitopes was performed because MPXV affects people globally.

2.6. Multiepitope Vaccine Construct Design. The final HTL, CTL, and LBL epitopes chosen were joined with linkers to create a vaccine design. While CTL epitopes were fused by the "AAY linker", HTL epitopes were connected using the "GPGPG linker". LBL epitopes that were left were joined by using the "KK linker". In the same vaccination design, which was linked via the "EAAAK linker", HBHA conserved was taken as an adjuvant to increase the immunogenicity of the vaccine. Additionally, a signal tPA peptide was added at the N-terminal to help transport the vaccine out of the cell.[42]

2.7. Analysis of the Vaccine Construct. Before the mRNA vaccine design was created, numerous factors were used to assess the vaccine construct. The instability index, aliphatic index, total positive and negative amino acids, molecular weight, GRAVY score, total number of amino acids in the query sequence, and the theoretical pI of protein vaccine design had been calculated using the Protparam server of Expasy.[43] Likewise, its antigenicity profile was also calculated using the Vaxijen v2.0 server, which has a predefined >0.4 threshold. The SOLpro server[44] had been utilized for the prediction of solubility during heterologous expression inside the host, and Allergenfp was used to evaluate the allergenicity. The optimum solubility overexpression level was maintained at >0.5.

2.8. Prediction of 2D and 3D Structures. The SOPMA server[45] was employed to design the peptide vaccine's secondary structure. Regions producing coiled, helical, and extended stranded structures were anticipated by using the provided server for computing. The Swiss Homology Modeling server[46] was applied to infer the tertiary structure, and the Galaxyrefine Web server[47] then refined it. Additionally, the Ramachandran plot in PROCHECK[48] and the quality factor at the ERRAT Web server were estimated to validate the structure's 3D quality.[49]

2.9. Prediction of Conformational B-Lymphocyte Epitopes. The solvent-accessible and surface-exposed B lymphocyte epitopes were determined, in addition to the conformational epitopes. The conformational B-cell epitopes validate a B-cell-linked immune response, so it is necessary to identify them in a three-dimensional vaccine construct. Using the Ellipro server, conformational B-cell epitopes in the vaccine construct were predicted and analyzed.[50]

https://doi.org/10.1021/acsomega.3c07866
ACS Omega 2023, 8, 43341−43355

2.10. Molecular Docking and Normal Mode Analysis. To evaluate the vaccine's affinity with humoral immune response cells, the vaccine design was docked with TLR2 (PDB ID: 2Z7X) and TLR4 (PDB ID: 3FXI) MHC molecules. The crystal structures of TLR2 and TLR4 that were needed for the investigation were downloaded from the protein data bank (PDB). Utilizing the MOE software tool, the protein structures were prepared for docking. Manual removal of water molecules and cocrystallized ligands was followed by the addition of H^+. Additionally, the energy of the protein structures was reduced using the MOE energy minimization algorithm tool. Using the conjugant gradient approach and the MMFF94x force field, the MOE determines the protein energy (in kcal/mol). The structures were saved in the .pdb format following predocking preparation.[51,52]

It has been demonstrated that methods based on the Fast fourier transform (FFT) are particularly efficient for predicting protein−protein interactions. The ClusPro 2.0 performs three algorithms, including the following method: FFT correlation approach for rigid body docking, root-mean-square deviation (RMSD)-based configuration clustering to identify the largest cluster that would accurately predict the model, and fine-tuning of targeted structures of the complex. Docking of the vaccine construct with TLR2 and TLR4 was done using ClusPro.[53] The resulting docked complexes were then visualized by using the Discovery Studio and Pymol software. After docking, the docked complexes were subjected to IMODs server for the normal-mode analysis to verify their stability.[54]

2.11. MD Simulation Studies. Molecular dynamics (MD) simulations for two receptors in complex with the designed vaccine were performed. For this analysis, the Schrödinger LLC's Desmond software was used.[55] These simulations lasted 100 ns for each system. Before the MD simulations start, an important preliminary step is docking the vaccine with receptors. It provides the first prediction of the static binding orientation of vaccine molecules in the active sites of the receptor. During MD simulations, Newton's classical equations of motion[56] were used to predict the dynamic vaccine-binding interactions in a physiological context by simulating the dynamic movements of individual atoms throughout time. The protein preparation wizard in Schrödinger's Maestro[57] was used to prepare the vaccine−receptor complexes for simulation studies. This preprocessing step included optimization, minimization, and adding any required residues that were missing to the system. The intermolecular interaction potential 3 points transferable solvent model was used in the simulations for the solvent environment.[58] This solvent model was used inside an orthorhombic simulation box with an OPLS_2005 force field, a 300 K temperature, and a 1 atm pressure. The simulation systems were given counterions and a sodium chloride concentration of 0.15 M to ensure the models' neutrality and to imitate physiological conditions. The models went through a relaxation or equilibration phase before the simulations started, during which the system's constraints were gradually loosened. The simulations' trajectories were captured and saved for later review. Finally, the stability of the vaccine−receptor complexes was investigated by examining the root-mean-square fluctuation (RMSF) and RMSD plots.

2.12. Immune Simulation Studies. To validate the immunological response more effectively to the peptide vaccine design, the C-ImmSim server[59] was utilized to run online dynamic immune simulation reports. A total of three doses (01, 84, and 168) were administered over the course of 4 weeks, each containing 1000 vaccine units and omitting LPS (1050). According to the reference, the other parameters were left as default.[60]

2.13. Vaccine Construct's Back-Translation and Codon Optimization. Using the JCAT[61] and ExpOptimizer tools,[62] we back-translated the vaccine construct into mRNA to facilitate its expression in the host (humans). The results' percentage of GC content and the effective translation capacity of mRNA were calculated using the codon adaptation index (CAI). The most optimized mRNA sequence was chosen, and the GenScript Web site's Rare Codon Analysis Tool was used to evaluate it. Here, the codon frequency distribution (CFD) factor served as a proxy for the existence of uncommon codons.

2.14. Design of mRNA Vaccine. The mRNA vaccine sequence was constructed by the following pattern:

"[5′ m7GCap-5′ UTR-Kozak sequence (containing start codon)-optimized mRNA [tPA (signal peptide)-EAAAK linker-HBHA conserved (Adjuvant)-PADRE sequence-GPGPG linker-HTL epitopes-KK linker-LBL epitopes-AAY linker-CTL epitopes-AAY linker-EAAAK linker]-Stop codon-$(3'UTR)_2$-Poly(A) tail 3′]"

In order to avoid degradation and promote translation, the 5′ cap was compromised in the development of the typical mRNA vaccine design. For enhanced translation efficacy, the beta-globulin protein's 5′ and 3′ UTR domains were inserted. A start-codon-containing sequence known as the Kozak sequence was also introduced. In order to boost RNA stability, the optimized mRNA sequence was inserted, followed by the addition of a poly(A) tail at the 3′ end.[63]

2.15. mRNA Vaccine Secondary Structure Prediction. In the biosynthesis of proteins, mRNA's secondary structure is essential. Its adverse impact on translation, which stops or obstructs ribosome initiation and action along the mRNA, can drastically reduce the protein yield, making it an important element in gene regulation. The minimal free energy calculation of the mRNA vaccine allows a variety of techniques to forecast the production of secondary structures. Here, the RNAfold and mfold Web servers were used to determine the secondary structure of the mRNA sequence.[64]

2.16. In-Silico Cloning. To ensure the efficiency of host-based expression, cloning of the designed vaccine construct was performed in *Escherichia coli* strain K12. For this purpose, reverse translation and codon optimization of the construct were performed by the Java Codon Adaptation tool.[65] Additional parameters such as rho-independent transcription terminators, prokaryotic ribosome-binding sites, and cleavage sites of restriction enzymes were avoided, and only partial optimization was selected to guarantee that the desired outcomes may be attained. After optimization, cloning of the vaccine construct was performed in the *E. coli* vector pET-28a using the Snapgene tool (https://www.snapgene.com/) by using a commercially available restriction site.[30,66]

2.17. Vaccines' Safety Profile Confirmation. In order to avoid any autoimmune response in the host, it is important to check the similarity of the vaccine construct with the human proteins. This was performed by a pBLAST of the vaccine construct against the human proteome, downloaded from the UniProt database.

https://doi.org/10.1021/acsomega.3c07866
ACS Omega 2023, 8, 43341−43355

Table 1. Analysis of MHC-I Interacting Epitopes

MHC-I alleles	start	end	MHC-I epitopes	score	rank	immunogenicity	antigenicity	Allergenfp	toxicity	conservancy
HLA-B*35:01	141	149	QPVKEKYSF	0.942536	0.02	−0.40888	antigen	allergen	non-toxin	100.00%
HLA-C*14:02	67	75	KYENPCKKM	0.501072	0.19	−0.34356	antigen	non-allergen	non-toxin	100.00%
HLA-B*35:03	23	31	VPTMNNAKL	0.702686	0.07	−0.26947	non-antigen	allergen	non-toxin	100.00%
HLA-B*14:02	308	316	DQYKFHKLL	0.688567	0.02	−0.26223	non-antigen	allergen	non-toxin	100.00%
HLA-B*40:01	91	99	YEVNSTMTL	0.981356	0.01	−0.24319	antigen	non-allergen	non-toxin	100.00%
HLA-A*30:02	259	267	KLSKDVVQY	0.84825	0.01	−0.24308	non-antigen	non-allergen	non-toxin	100.00%
HLA-C*08:02	47	55	TCDSGYHSL	0.935523	0.03	−0.19911	non-antigen	allergen	non-toxin	100.00%
HLA-A*68:01	35	43	ETSFNDKQK	0.816131	0.2	−0.171	antigen	allergen	non-toxin	100.00%
HLA-B*44:03	111	119	EEKNGNTSW	0.980939	0.01	−0.1135	antigen	non-allergen	non-toxin	100.00%
HLA-B*48:01	183	191	QQKCDIPSL	0.46105	0.05	−0.08339	antigen	allergen	non-toxin	100.00%
HLA-A*01:01	78	86	VSDYVSELY	0.996027	0.01	−0.03403	non-antigen	allergen	non-toxin	100.00%
HLA-C*15:02	2	10	KTISVVTLL	0.87381	0.01	−0.01793	antigen	allergen	non-toxin	100.00%
HLA-B*53:01	58	66	NAVCETDKW	0.57593	0.09	−0.01409	non-antigen	allergen	non-toxin	100.00%
HLA-B*58:01	222	230	SSTCIDGKW	0.714383	0.17	0.01143	antigen	non-allergen	toxin	100.00%
HLA-A*02:03	282	290	IMALTIMGV	0.676557	0.11	0.03622	antigen	allergen	non-toxin	100.00%
HLA-A*02:01	292	300	FLISIIVLV	0.8569	0.05	0.15997	antigen	allergen	non-toxin	100.00%
HLA-A*29:02	**160**	**168**	**GYEVIGVSY**	**0.700535**	**0.09**	**0.17372**	**antigen**	**non-allergen**	**non-toxin**	**100.00%**
HLA-A*68:02	272	280	ESLEATYHI	0.742411	0.07	0.18757	antigen	allergen	non-toxin	100.00%
HLA-C*03:03	**201**	**209**	**FSIGGVIHL**	**0.934996**	**0.01**	**0.28038**	**antigen**	**non-allergen**	**non-toxin**	**100.00%**

Table 2. Analysis of MHC-II Interacting Epitopes (the Rows in Bold Show the Selected Epitopes)

MHC-II alleles	start	end	MHC-II epitopes	rank	antigenicity	toxicity	allergnfp	IFN gamma Induction	IL4 Induction	IL10 Induction	conservancy
HLA-DPA1*03:01/DPB1*04:02	**286**	**300**	**TIMGVIFLISIIVLV**	**0.47**	**antigen**	**non-toxin**	**non-allergen**	**positive**	**non IL4 inducer**	**IL10 inducer**	**100.00%**
HLA-DRB3*02:02	**88**	**102**	**KPLYEVNSTMTLSCN**	**0.99**	**antigen**	**non-toxin**	**non-allergen**	**positive**	**non IL4 inducer**	**IL10 noninducer**	**100.00%**
HLA-DRB1*01:01	**48**	**62**	**CDSGYHSLDPNAVCE**	**1.3**	**antigen**	**non-toxin**	**non-allergen**	**negative**	**IL4 inducer**	**IL10 noninducer**	**93.33%**
HLA-DQA1*05:01/DQB1*03:01	190	204	SLSNGLISGSTFSIG	1.4	non-antigen	non-toxin	non-allergen	no data	non IL4 inducer	IL10 noninducer	100.00%
HLA-DQA1*05:01/DQB1*02:01	**264**	**278**	**VVQYEQEIESLEATY**	**1.5**	**antigen**	**non-toxin**	**non-allergen**	**no data**	**IL4 inducer**	**IL10 noninducer**	**100.00%**

Table 3. Analysis of Predicted B-Cell Epitopes[a]

B-cell epitopes	start	end	score	antigenicity	allergenicity	toxicity	conservancy
CQPLQLEHGSCQPV	**130**	**143**	**0.886**	**antigen**	**non-allergen**	**non-toxin**	**100.00%**
KNGNTSWNDTVTCP	**113**	**126**	**0.89**	**antigen**	**non-allergen**	**non-toxin**	**100.00%**
TLTGSPSSTCIDGK	**216**	**229**	**0.932**	**antigen**	**non-allergen**	**non-toxin**	**100.00%**
EEFDPVDDGPDDET	242	255	0.983	antigen	allergen	non-toxin	100.00%
SKDVVQYEQEIESL	261	274	0.984	non-antigen	non-allergen	non-toxin	100.00%

[a]The rows in bold show the selected epitopes.

3. RESULTS

3.1. Determining Consensus Sequence from MSA. All retrieved protein sequences were aligned using Clustal W, and it was found that most of the amino acid sequences were conserved. The MSA aligned file was used by using Bioedit software to create a consensus sequence. Afterward, consensus sequences of all the proteins were analyzed, and the final EEV Type-I membrane glycoprotein was selected for the vaccine design (Table S1).

3.2. T-Lymphocyte Epitope Prediction. Using the NetMHCpanEL 4.1 tool, 19 unique CTL epitopes were discovered by utilizing a thorough reference set of HLA alleles. Of these, six epitopes were identified as immunogenic. The T-cell epitopes were then subjected to a population conservancy analysis, showing a complete range of conservancies of more than 90%. Two epitopes were chosen as the best epitopes to use in the final peptide-based vaccine design after they were analyzed for their nontoxicity, nonallergenicity, and antigenicity (Table 1).

The prediction findings for MHC-II epitope analysis identified five distinct epitopes with an adjusted rank of less than 2.0 since the lower percentile rank denotes high interaction affinity. All epitopes were found to be conserved after being subjected to a conservancy analysis. These epitopes were also tested for their antigenicity, nonallergenicity, and nontoxicity. Using the IL10pred and IL4pred servers, the IL-10 and IL-4 inducing capabilities of these epitopes were also studied, respectively. The analysis resulted in the selection of four epitopes for vaccine design (Table 2).

3.3. Population Coverage Analysis. The population coverage of the selected T cell epitopes was evaluated using the IEDB population coverage tool. The results of the population

https://doi.org/10.1021/acsomega.3c07866
ACS Omega 2023, 8, 43341−43355

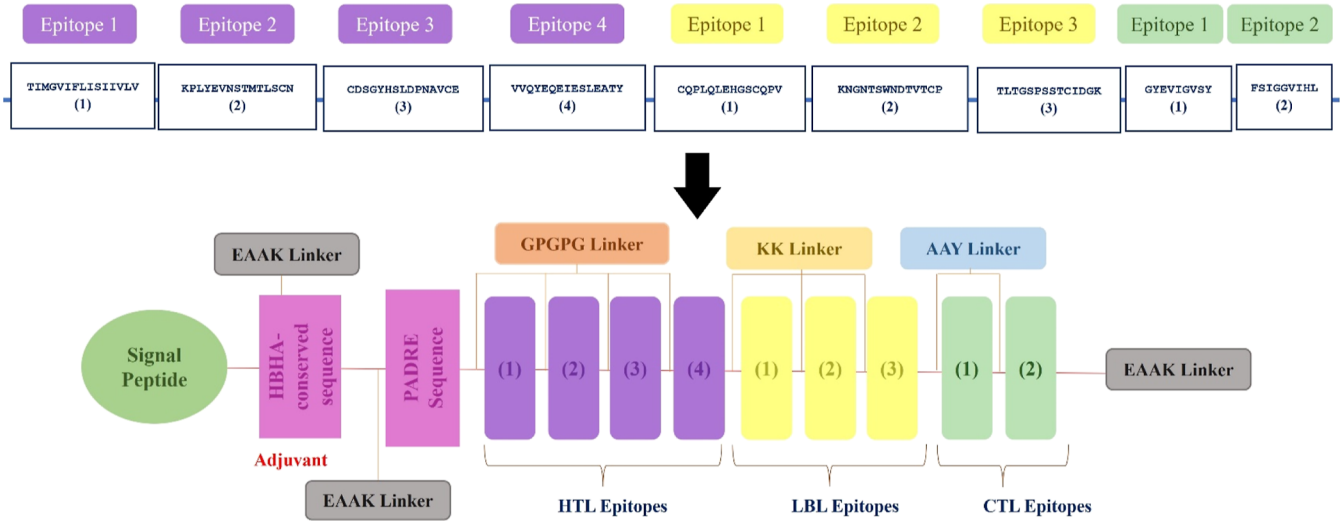

Figure 2. Schematic presentation of the vaccine design including sequences of the selected HTL, LBL, and CTL epitopes, with bracketed numerals showing their placement in the final vaccine construct. Lastly, there is an overview of the final vaccine construct with adjuvants, linkers, and epitopes of the final multiepitope MPXV Vaccine construct.

coverage of our selected MHC-I and MHC-II epitopes concluded that our epitopes cover 100% of the world's population, which indicated that the vaccine will be beneficial for the people present all around the world. The overall population coverage of the epitopes is depicted in Figure S1.

3.4. B-Lymphocyte Epitope Determination. The BCPRED server analysis led to the selection of five possible B-cell epitopes for an additional study. Based on their antigenic, nontoxic, conservancy, and nonallergenic profiles, three epitopes were selected for further analysis (Table 3).

3.5. Construction and Analysis of the Peptide Vaccine. The final selection of 3 linear B-cell, 2 CTL, and 4 HTL epitopes was used in this vaccine design. The vaccine design also included the tPA signal peptide, linkers, and adjuvants. To enhance the immunological response, the adjuvant was also included in the vaccine construct (Figure 2). Through the ProtParam server, the physiochemical characteristics of the predicted vaccine construct using hypothesized epitopes were assessed. In addition, calculations were made for additional variables such as antigenicity, allergenicity, and solubility under overexpression (Table 4).

3.6. Prediction of 2D and 3D Structures of the Peptide Vaccine Construct. The SOPMA server was used to determine the secondary structure of the designed vaccine construct. The projected structure has been shown to contain a 22.73% random coil structure, 17.05% extended strand, 3.98% beta turn, and 56.25% α helix. Utilizing the Swiss Model server, the model of vaccine constructs was created and further refined using the GalaxyRefine Web server. Tertiary structure verification is important since it uncovers probable mistakes in anticipated 3D models. Pymol and Discovery Studio were used for the visualization of the vaccines' tertiary structure. The ERRAT server verified the predicted 3D structure, and the quality factor it returned was "99.34", confirming the structure's high quality. To confirm the precise 3D structure, we also used the Ramachandran plot validation parameter was also used. The Ramachandran plot shows the percentage of residues in favorable, forbidden, and allowed areas, which describes the model's quality. The SAVES Web site was used to expose the improved 3D structure to the Ramachandran plot analysis, and the results revealed that 94.4, 4.6, and 0.5%

Table 4. Characteristics Analysis of the Peptide Vaccine Construct

sr. no.	physiochemical properties	measurement	indication
1	total number of amino acids	247	appropriate
2	molecular weight	26002.27	appropriate
3	theoretical pI	8.95	basic
4	total number of negatively charged residues (Asp + Glu)	18	
5	total number of positively charged residues (Arg + Lys)	29	
6	aliphatic index (AI)	79.8	thermostable
7	grand average of hydropathicity (GRAVY)	−0.036	hydrophilic
8	antigenicity (using VaxiJen)	0.5272	antigenic
9	solubility upon overexpression (using SOLpro)	0.843579	soluble
10	allergenicity (using Allergenfp)	nonallergen	non-allergenic
11	instability index	30.16	stable

of the residues were in preferred, allowed, and forbidden regions, respectively. The findings show that the three-dimensional structure is of good quality (Figure 3).

3.7. Conformational B-Cell Epitope Prediction. In the designed vaccine construct, the conformational B-cell epitopes were likewise predicted by the Ellipro server. Three conformational LBL epitopes in total were found in the vaccine design, demonstrating the vaccine's potent capacity to activate B-cell responses (Table S2).

3.8. Molecular Docking and Normal Mode Analysis. ClusPro was employed for interaction studies between the peptide vaccine constructs and receptors. For the TLR2 receptor, the best complex model contained the highest center score of −1006.4 kcal/mol and the lowest energy of −1137.0 kcal/mol. As compared to TLR2, the TlR4-resulting complex showed even greater interaction, with the highest binding score of −1333.8 kcal/mol and the lowest energy of −1342.6 kcal/mol. On the basis of their lower energy scores, it was predicted that these complexes, especially with TLR4, have strong binding affinity. Pymol was used for the visualization of the docked complexes and their interactions (Figure 4A & 5A).

https://doi.org/10.1021/acsomega.3c07866
ACS Omega 2023, 8, 43341−43355

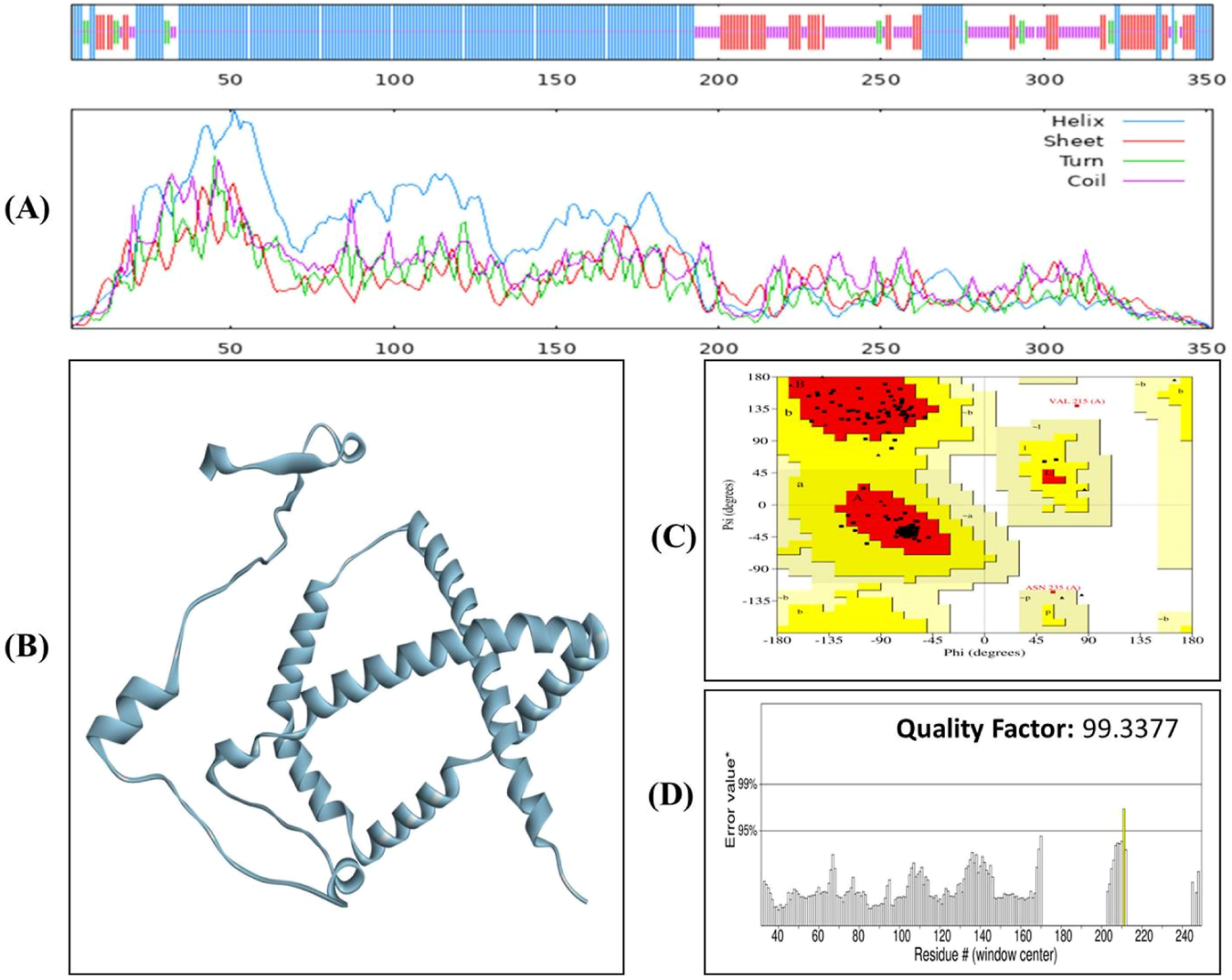

Figure 3. (A) Secondary structure of the vaccine formed by the SOPMA server. (B) Vaccine 3D structure modeled by Swiss model and refined using the Galaxyrefine server. (C) Ramachandran plot exhibiting 93.9% in the Rama-favored region. (D) ERRAT graph indicating a quality factor value of 99.33.

The normal-mode analysis (NMA) was carried out to determine the molecular stability and functional movements of the vaccine−receptor complexes (Figures 4 and 5). The major chain deformed region residues in the vaccine−receptor complexes were shown by peak points on the deformability graph. The "hinges/linkers" in the main chain can be identified using the high deformability regions (Figures 4B and 5B). The experimental B-factor plot, which represents the average RMSD values of the docked complex, shows the correlation between NMA mobility and the vaccine−receptor complexes (Figures 4C and 5C). The vaccine−TLR2 and vaccine−TLR4 complex's estimated eigenvalues were 2.919077×10^{-6} and 9.999751×10^{-7}, respectively, which represents the motion stiffness associated with each normal mode (Figures 4D and 5D). Individual (purple) and cumulative (green) variances are shown for each normal mode of the complex in the variance bar. The correlation between variance and eigenvalue was negative (Figures 4E and 5E). A covariance map additionally depicts the motions that interact between two molecules inside a complex. In the current investigation, correlated (red), uncorrelated (white), and anticorrelated (blue) atomic motions in the vaccine−receptor complexes were used to describe linked motions among various pairings of residues (Figures 4F and 5F). Additionally, a specific electric network map that depicts the vaccine−receptor complex's pair of atoms connected by springs was produced. The stiffness and assembly between comparable atoms of bigger molecules are shown by colored dots, and rigid springs are represented by darker gray (Figures 4G and 5G). A stable interaction between the receptors and the designed vaccine was eventually predicted by NMA analysis.

3.9. MD Simulations. For molecular dynamic simulations, Schrödinger LLC's Desmond software was used. The simulation time was 100 ns for both complexes; vaccine−TLR2 and vaccine−TLR4. The RMSD in the bound and unbound states of the vaccine and receptors TLR2 and TLR4 was calculated and presented as a histogram against the Ca atoms of the protein for interpretation of the conformational stability and dynamic properties from the initial configuration to the final state (Figure 6). Minor deviations from the RMSD curve imply the stability of the docked complex and vice versa, like in the present case, i.e., the vaccine in complex with the TLR2 and TLR4 receptors. In the case of the vaccine−TLR2 complex, the RMSD calculated was 9.5 Å ± 1 Å and showed

https://doi.org/10.1021/acsomega.3c07866
ACS Omega 2023, 8, 43341−43355

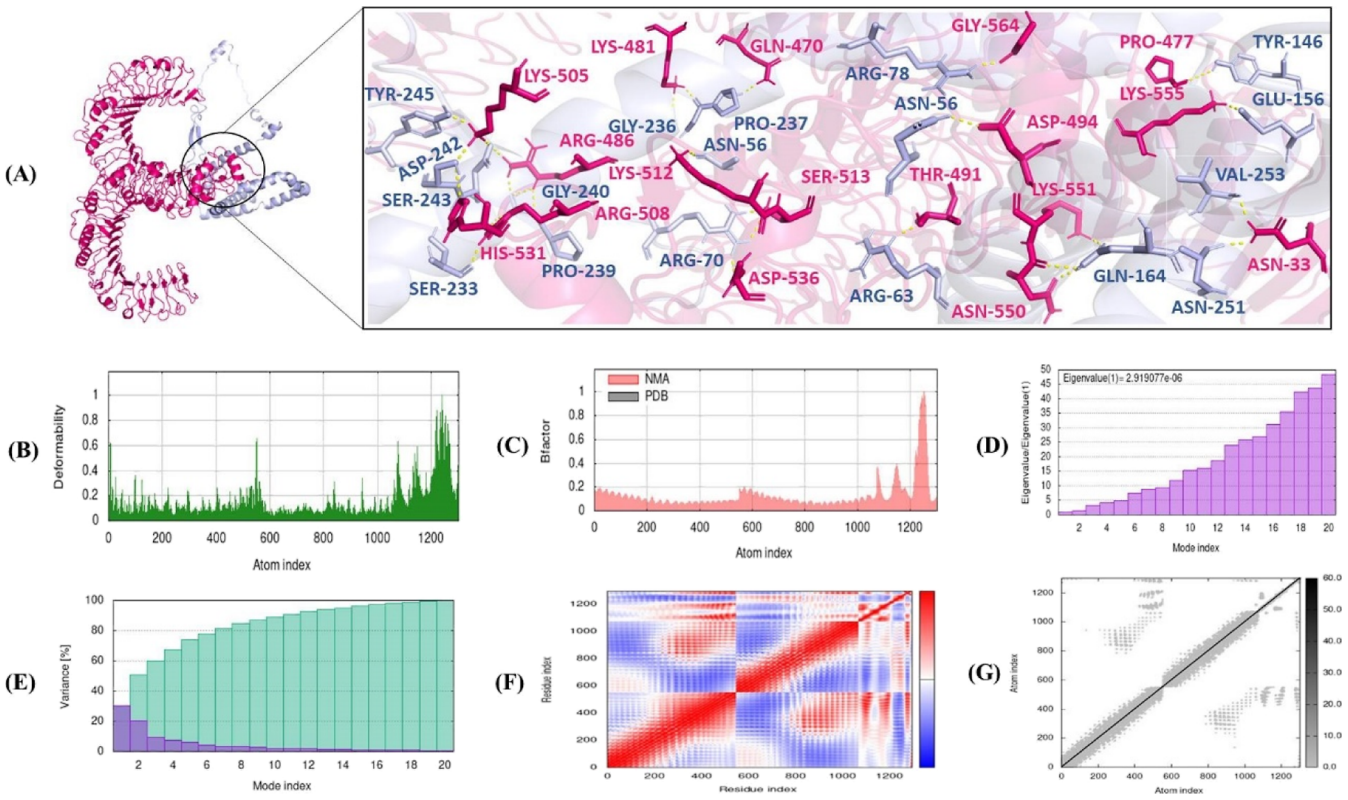

Figure 4. (A) Interaction analysis of vaccine (light-blue) and TLR2 (pink) complex. (B) Deformability. (C) B-factor. (D) Eigenvalue. (E) Variance map. (F) Covariance map. (G) Elastic network model.

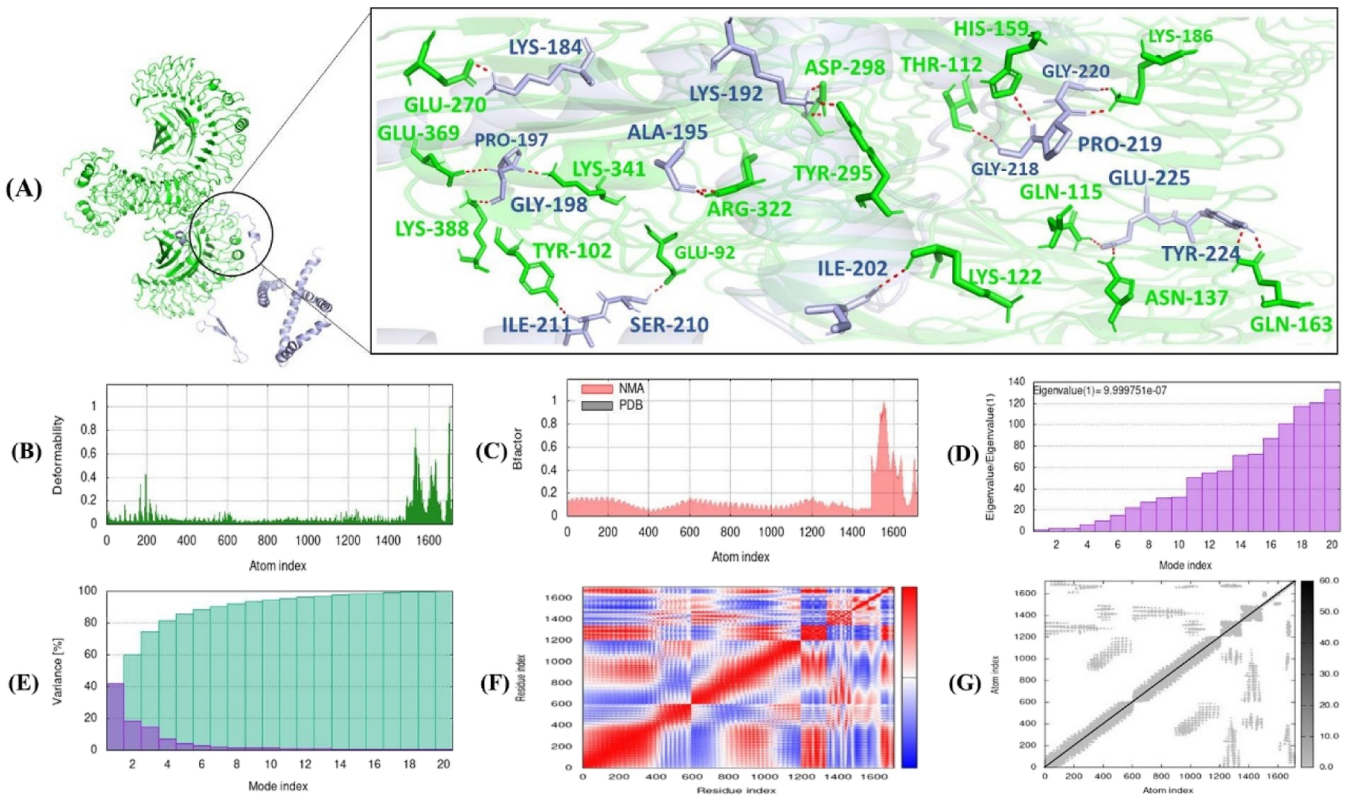

Figure 5. (A) Interaction analysis of vaccine (light-blue) and TLR4 (green) complex. (B) Deformability. (C) B-factor. (D) Eigenvalue. (E) Variance map. (F) Covariance map. (G) Elastic network model.

no substantial variation after convergence during the whole simulation period except initial fluctuations between 0 and 40 ns (Figure 6A), while in the case of the vaccine−TLR4 complex, the calculated RMSD was 12.0 Å ± 1 Å and showed

https://doi.org/10.1021/acsomega.3c07866
ACS Omega 2023, 8, 43341−43355

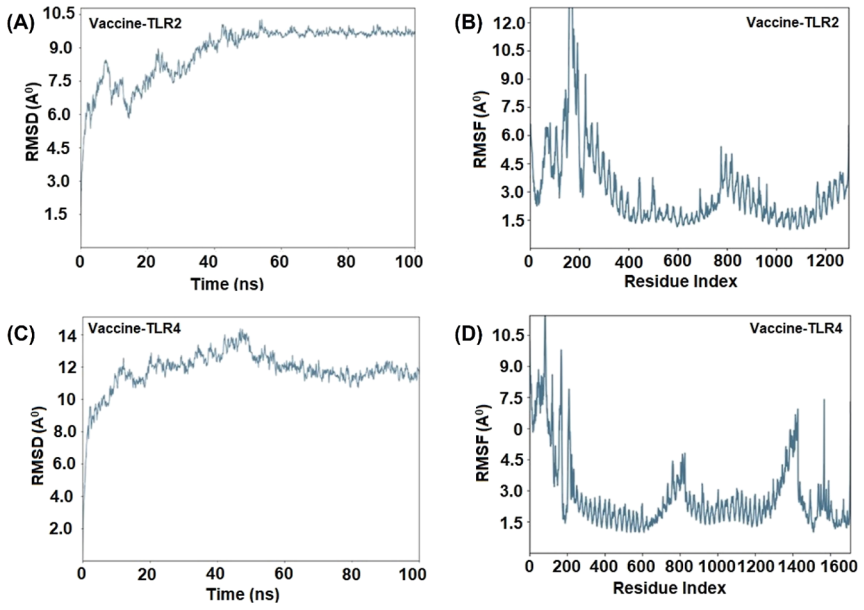

Figure 6. RMSD and RMSF plots for receptors and the vaccine construct complex. (A) RMSD plot of the vaccine−TLR2 complex. (B) RMSF plot of the vaccine−TLR2 complex. (C) RMSD plot of the vaccine−TLR4 complex. (D) RMSF plot of the vaccine−TLR4 complex.

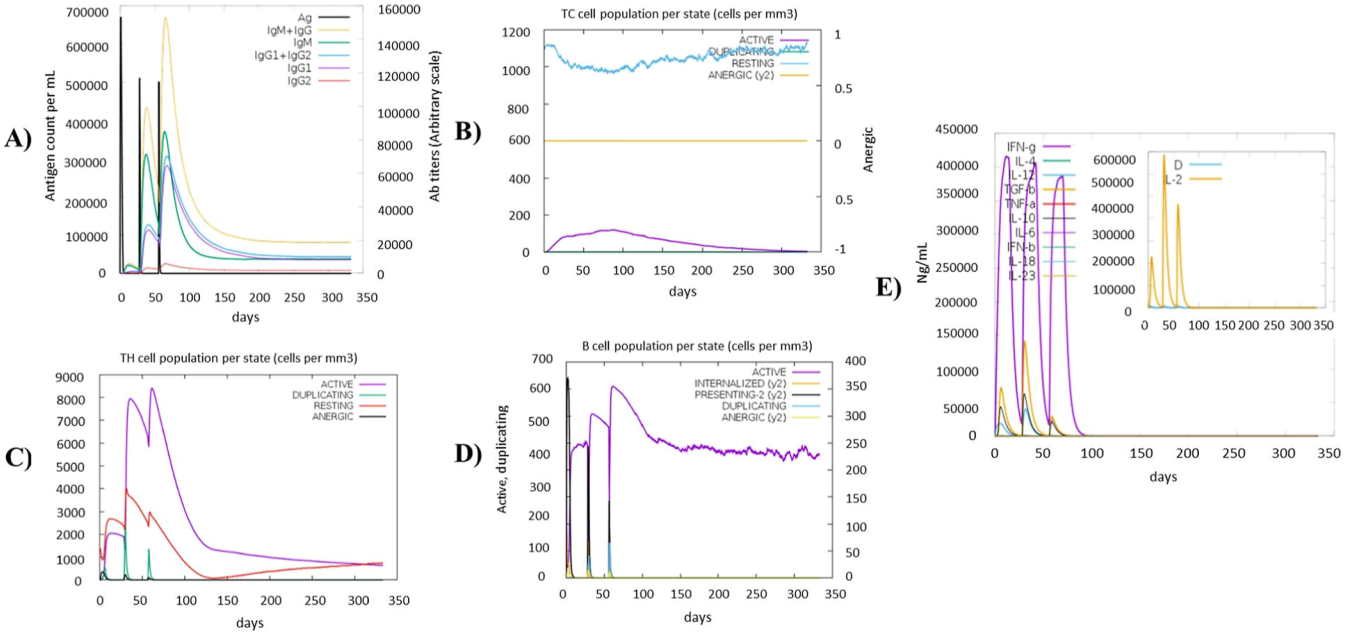

Figure 7. Immune simulation results of the designed MPXV vaccine construct. (A) Immunoglobulin levels with respect to antigen concentration. (B) Cytotoxic T-cell population per state. (C) Helper T-cell population per state. (D) B-cell population per state. (E) Production of cytokine and interleukins with Simpson index.

slight variations until 45 ns except some sudden variations at 18 and 42 ns. After that, no significant variations were identified (Figure 6C). The RMSD plots of both the TLR2 and TLR4 docked complexes indicated their stability. The observed heightened fluctuations in RMS values in both complexes can be attributed to the presence of inherently flexible regions.[67,68] This is notably correlated with the inclusion of loop regions where epitopes and linker sequences have been inserted in addition to the tPA signal peptide and adjuvants affixed at the N-terminus. This prominent fluctuation trend is consistent with the findings reported by previous studies[69,70] as well as supporting the notion of structural dynamics in this context.

The local alterations along the protein chain can be characterized using RMSF. In the RMSF plots, regions of the protein that fluctuate the greatest during the simulations are indicated by peaks. Therefore, we performed the residual flexibility analysis to better understand the stability of the formed complexes, which indicated that both the TLR2 and TLR4 receptors have lower values of flexibility (Figure 6B,D), which confirm our analysis.

3.10. Immune Simulation. The C-IMMSIM server was used to check the immunological simulation profile (Figure 7). The first graph (A) shows the IgM and IgG primary antibody responses, with the IgM + IgG rate dramatically rising after the third injection of the vaccination. Positive immunological

https://doi.org/10.1021/acsomega.3c07866
ACS Omega 2023, 8, 43341−43355

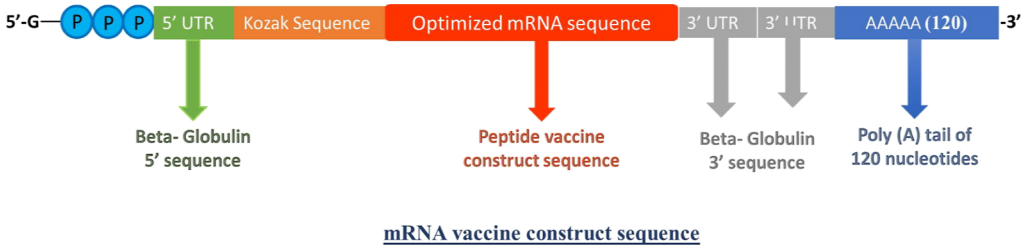

Figure 8. Illustration of the designed MPXV mRNA vaccine construct.

outcomes are indicated by graphs (B) and (C), which demonstrate a significant rise in the generation of cytotoxic and helper T-cells. The B-cell graph (D) showed that the immune response is active and consistently high after the third injection. The interleukin levels and danger level "D" are shown in the last graph (E), where the apex for risk is too low, indicating a favorable reaction to vaccination.

3.11. Optimized mRNA Determination Prediction of the Secondary Structure. The ExpOptimizer tool and Jcat (Java Codon Adaptation Tool) were both utilized to achieve codon optimization. Further evaluation of these techniques' outputs was done using GC content (%) and the CAI. The JCAT tool's optimized mRNA sequence displayed a suitable GC content range and a high CAI score (Figure S3). With the use of the GenScript server's Rare Codon Analysis Tool, this optimized mRNA was further confirmed. There, the factor CFD, which ended up being 0.00%, determined the absence of any uncommon codon. This demonstrated the improved mRNA sequence's excellent overall translation effectiveness (Table S3).

3.12. Predicted mRNA Vaccine Sequence. The predicted mRNA vaccine sequence was constructed as a **5′** m7GCap-5′ UTR-Kozak sequence (containing start codon)-Optimized mRNA [tPA (Signal peptide)-EAAAK-HBHA conserved (Adjuvant)-PADRE sequence-GPGPG-TIMGVI-FLISIIVLV-GPGPG-KPLYEVNSTMTLSCN-GPGPG-CDSGYHSLDPNAVCE-GPGPG-VVQYEQEIESLEATY- KK-CQPLQLEHGSCQPV-KK-KNGNTSWNDTVTCP-KK-TLTGSPSSTCIDGK-AAY- GYEVIGVSY-AAY-FSIGGVIHL-AAY-EAAAK linker]-Stop codon-$(3'UTR)_2$-Poly(A) tail (120 bases) **3′**

In the design, the 3′ and 5′ beta-globin UTRs will increase translation efficiency, the Kozak sequence will serve as the protein translation initiation site in many eukaryotic mRNA transcripts, and the tpa signal sequence will direct the target protein into the cellular secretion pathway. The 5′-Cap will halt the degradation of mRNA to facilitate the binding of the translation factor. At the 3′ end of the mRNA, a poly(A) tail of 120 bases was added to increase stability and translation rate (Figure 8).

3.13. Prediction of the Secondary Structure. The secondary structure prediction was carried out by utilizing the mfold and RNAfold servers. The mRNA sequence was folded in multifold, yielding a free energy of "−438.00 kcal/mol". The overall free energy value provided by the RNAfold was "−444.96 kcal/mol", which is near the mfold value and thus predicted a secondary structure of good quality (Figure S3).

3.14. In Silico Cloning and Safety Analysis of the Vaccine. Reverse translation and codon optimization of the vaccine construct were performed using the Jcat server. After then, the in silico cloning was performed to check how MPXV behaves in the *E. coli* strain K12 expression system. pET-28a was used as a vector, and the vaccines' optimized sequence was inserted into it by using the commercially available restriction site Nru1 by using the Snapgene software (Figure S4). To ensure the safety profile of the designed vaccine, we performed its pBLAST against *Homo sapiens*, which resulted in zero homology of our vaccine with any human protein. This indicates that our vaccine is absolutely safe for use, and there may be no chance of autoimmune response after administration of the designed vaccine.

4. DISCUSSION

Since the eradication of smallpox in the early 1980s, the World Health Organization has determined that MPXV is the main orthopox virus impacting human populations. MPXV is the next most deadly type of orthopox virus that affects humans, following the smallpox virus. Most of the medical symptoms of a monkeypox infection in humans are similar to those of smallpox. Generalized headaches and exhaustion follow a feverish prodrome at first. Many individuals have maxillary, cervical, or inguinal lymphadenopathy (diameter of 1−4 cm) before and concurrent with the development of the rash. The WHO established standards for suspected cases of monkeypox by January 1, 2022. Any person who exhibits an intense skin rash or lesion along with a preliminary sign of monkeypox meets the criteria. An individual is thought to be a probable monkeypox case if another reason cannot account for their presenting symptoms.[71] Monkeypox rash typically starts on the face, moves down the body, and affects the soles and palms of the hands. The current outbreak's rash pattern is a little odd, though. Bleeding, anal pain, and not even a single lesion were all reported in various investigations. Large lymph nodes are hard, sensitive, and occasionally uncomfortable. Smallpox was not characterized by lymphadenopathy.[9]

Monkeypox is often a benign condition that rarely needs supportive treatment. Some people, however, run the danger of contracting a serious illness that necessitates hospitalization and medical care. Both people who are at a high risk of contracting a serious illness, and those who are currently doing so are advised to receive treatment with antiviral medications. For monkeypox, no particular antiviral medications were created. In the past, only three antiviral medications Tecovirimat, Cidofovir, and Brincidofovir among the numerous that were prescribed for the treatment of smallpox were known to be successful in treating the MPXV. Monkeypox has been treated using Vaccinia immunoglobulin, which was initially created to address the side effects of Vaccinia vaccination. The antiviral treatments for smallpox, however, have been demonstrated to be less effective and are unable to stop the spread of MPXV from asymptomatic patients to healthy individuals.[72]

The resistance against orthopox viruses has been declining since the smallpox vaccination programs were discontinued

https://doi.org/10.1021/acsomega.3c07866
ACS Omega 2023, 8, 43341−43355

after the disease was eradicated. Additionally, there are animal reservoirs for the MPXV. These characteristics collectively make it difficult to stop the spread of monkeypox. Moreover, there has been no vaccine developed for treating MPXV. The modified Vaccinia Ankara and ACAM2000 vaccines were previously used for vaccination against monkeypox; however, they are not effective for every individual. The adverse effects that people encounter range from minor ones that endure for 1 to 2 weeks (such as chills and fever, localized pain and erythema, weariness, and aches in the muscles) to severe ones (like pericarditis, encephalitis, and myocarditis). In this case, safe and dependable MPXV immunity building could greatly aid in the total eradication of the virus.[73]

mRNA vaccines are an emerging therapeutic approach with the benefits of high safety and efficacy as well as easy production and, therefore, have been extensively used in treating a variety of human diseases, including malignant tumors.[74] Additionally, mRNA vaccines have some built-in restrictions. The mRNA of vaccines may also break down quickly after injection and trigger cytokine storms. This poses a significant obstacle to mRNA delivery. However, the use of the appropriate carriers can prevent degradation and improve biosafety, effector presentation, immunological responses, and biocompatibility.[75] Due to their amazing benefits over other forms of nucleic acids and traditional vaccinations, nucleic acid vaccines, particularly mRNA-based vaccines, have recently attracted a lot of attention. mRNA vaccines are quickly produced and extremely efficient, safe, and economical. Various mRNA vaccines developed against Zika, HIV-1, influenza, rabies, and many more viruses have represented a practical and remarkable subset of vaccinations since the first successful case of mRNA therapies in 1990.[76] Compared to the dormant virus vaccine that is now available, the predicted mRNA vaccine design has the potential to be more generally approved. The reason is that due to its modular nature, it is easy to customize the mRNA vaccines by the alteration of the sequence which encodes the target antigen.[77] RNA vaccines have been found to be effective in many infectious diseases such as rabies, AIDS, and malignancies.[78] They are better than the other types of vaccines because they can be quickly designed and tested and are highly immunogenic. They are safe to use as they do not contain live viruses but contain only antigenic parts, which are able to induce a potent immune response.[78] Once delivered into the host cells, the proteins are translated into the desired target proteins. The environment of the cell is then used to digest the proteins. The produced antigenic peptides are transported to the cell surface by MHC molecules in order to elicit a strong T-cell-mediated immune response. Helper T cells hasten the elimination of the circulating pathogens by stimulating the B cells to produce neutralizing antibodies. Additionally, helper T cells' production of inflammatory cytokines like interferon gamma causes phagocytes to become activated (IFN-c).[79]

In this study, the mRNA vaccine against MPXV infections was developed using an MPXV EEV type-I glycoprotein. The conserved EEV type-I glycoprotein sequence was originally created using in silico techniques, after which immunoinformatic analysis was employed to create the vaccine sequence. The IEDB analysis and numerous other characteristics, such as antigenicity, allergenicity, conservancy, and toxicity analyses, were used to determine the T- and B-cell epitopes. The IFN-gamma, IL-4, and IL-10 inducing properties of only MHC-II molecules were checked because they play a critical role in the production of these cytokines by presenting the pathogen-specific antigens to the helper T-cells. These properties could not be determined for MHC-I molecules because they do not interact with the helper T-cells but instead interact with cytotoxic T-cells to kill the died or abnormal cells.[80]

Linkers play an essential role in joining the epitopes and help in the proper functioning of the vaccines.[81] Following a rigorous investigation, different linkers (AAY, GPGPG, and KK) were used to connect the finalized B- and T-cell epitopes in order to create a vaccine construct.[30,49] These linkers are immunogenic and boost the immunogenicity of the designed vaccines. Furthermore, linkers help prevent the epitope-folding and keep the epitopes separated from each other.[82] A typical form of a linker for joining two protein domains is the AAY linker. It has been demonstrated that this linker improves the immunological response to vaccination antigens by making the antigenic sites more accessible to immune cells. Additionally, it supports the vaccine's antigens' structural integrity.[83] Another popular linker in vaccine design is the GPGPG linker. The antigens of the vaccine can be folded easily due to the flexibility of this linker. Additionally, it aids in reducing antigen aggregation, which can compromise the antigen's immunogenicity and stability.[84] A protein antigen is frequently joined to a carrier protein, such as a bacterial toxin, by using the KK linker. A more robust immunological response is produced as a result of the linker's positive charge stabilizing the contact between the antigen and carrier protein.[85] Furthermore, EAAAK, an empirical-helical linker, was employed to increase the stiffness, boost the stability of the fusion protein, and improve the bifunctional catalytic activity.[83] An HBHA conserved adjuvant, which has been recognized as an effective and beneficial adjuvant, was also added to the vaccine sequence to boost the immunogenicity of the designed vaccine.[86] This adjuvant stimulates the TLR4 protein and causes a number of immunological reactions.[87] The tPA signal sequence was also added to boost antigen secretion and expression.[88] A pan HLA-DR epitope peptide called the PADRE sequence was employed in the construction of the vaccine to increase its potency with minimal toxicity.[89]

Different in silico servers predicted and validated the secondary and tertiary structures of the designed construct. The vaccine construct was docked with the TLR2 (PDB ID: 2Z7X) and TLR4 (PDB ID: 3FXI) immunological receptors, which are widely present in humans, and subjected to MD simulation studies for 100 ns to verify the stability of the vaccine complexed with these receptors. After all of the confirmation, the vaccine design was then tested using the C-IMMSIM server to determine the immune response, which builds an immunological profile based on injections given at various intervals. Due to the immunological profile's heightened T- and B-cell responses, this vaccine construct was used in the development of the mRNA vaccination sequence. The mRNA vaccine sequence was created using a variety of sequences, including the 5′ cap, the 5′ and 3′ UTR regions, the poly(A) tail, and the back-translated vaccine construct. For the creation of the vaccine, the 5 and 3′ UTR regions are crucial. These areas are crucial for increasing the mRNA's ability to translate well. The study's findings showed that the expression of the protein was prolonged in mRNA with a poly(A-tail) of 120 lengths. We selected cap 1 (7-methyl-GpppN20-*O*-methyl) for the 5′ end-capping. By combining the 3′ end poly A tail and the 5′ cap, we are able to lengthen the half-life of the mRNA in this way. The

https://doi.org/10.1021/acsomega.3c07866
ACS Omega 2023, 8, 43341−43355

translation of the vaccine was additionally enhanced by the inclusion of the Kozak sequence. The signal peptide produced by the human tissue plasminogen activator is another amino acid chain (tPA). The tPA signal sequence enhances the immunogenicity of the vaccination. Additional invitro and in vivo research is required to examine the commercial application of generated mRNA sequences. Unquestionably required is in vivo verification of the safety and effectiveness of the potentially ubiquitous mRNA vaccine that was developed and tested in silico in this study. The experiment involving animal immunization should then be carried out to evaluate the immunological reactions. The goal of this project is to hasten and accurately produce an MPXV vaccine that will be useful for future vaccine development.

Although some other studies also focused on designing an immunoinformatics-based vaccine against MPXV, the proteins utilized in these studies are different from the protein used in this study.[68,90,91] In a similar study, the EEV Type-I membrane glycoprotein was used, but the predicted epitopes are different to those predicted in this study.[91] Similarly, another study predicted the epitope "FSIGGVIHL" and used it for the formulation of the vaccine against MPXV; however, our designed vaccine binds more strongly with the human toll-like receptors as compared to the vaccine designed in that study.[68] Furthermore, the vaccine designed in this study is effective for individuals worldwide because the epitopes of vaccine covered 100% of the world population. The designed vaccine is safe for use in humans because it does not show any similarity to human proteins. The quality of our vaccine 3D formed by Swiss Model server verified by the ERRAT quality factor also indicated the very good quality of the designed structure as no error was found in the structure. All these analyses indicated that the vaccines designed in this study are worthy of experimental validation to combat the deadly virus.

5. CONCLUSIONS

The ongoing monkeypox outbreak and higher infection rates are becoming a worldwide concern. To diagnose patients early and stop the spread of the virus further, mutual efforts are required. Additionally, vaccinations for contacts, researchers, and healthcare professionals are needed. Being very deadly, it was suggested that an effective vaccination method be proposed for its cure. Thus, we had proposed an mRNA-based vaccine for treatment of monkeypox in our study using an in silico method. Our study successfully designed a multiepitope mRNA vaccine as an effective candidate against MPXV infection. However, it should be tested and determined by meticulous in vitro, in vivo, and clinical studies for further validation of its efficacy. Our studies may aid in building a potential future MPXV vaccine in the coming years.

■ ASSOCIATED CONTENT

Supporting Information

The Supporting Information is available free of charge at https://pubs.acs.org/doi/10.1021/acsomega.3c07866.

Physiochemical and general properties analysis of vaccine candidate proteins for MPXV; Conformation of B-cell epitopes' prediction using the Ellipro server; analysis of the mRNA sequence by codon optimization tools; population coverage analysis of the T-cell epitopes performed by the IEDB tool; codon optimization of the vaccine construct done by ExOptimizer and the Jcat tool, indicating the optimized relative adaptiveness, GC-content, and vaccine sequence after adaptation; secondary structure of the mRNA vaccine construct; and in silico cloning of the designed vaccine into E. coli pET-28a vector performed by the SnapGene tool (PDF)

■ AUTHOR INFORMATION

Corresponding Authors

Mohibullah Shah − *Department of Biochemistry, Bahauddin Zakariya University, Multan 66000, Pakistan;* orcid.org/0000-0001-6126-7102; Phone: +92-313-9712930; Email: mohib@bzu.edu.pk, mohibusb@gmail.com; Fax: +92-61-9210071

Suvash Chandra Ojha − *Department of Infectious Diseases, The Affiliated Hospital of Southwest Medical University, 646000 Luzhou, China*; Phone: +86 158 8238 2103; Email: suvash_ojha@swmu.edu.cn

Authors

Samavia Jaan − *Department of Biochemistry, Bahauddin Zakariya University, Multan 66000, Pakistan; School of Biochemistry and Biotechnology, University of the Punjab, Lahore 54590, Pakistan*

Muhammad Shehroz − *Department of Bioinformatics, Kohsar University Murree, Murree 47150, Pakistan*

Asifa Sarfraz − *Department of Biochemistry, Bahauddin Zakariya University, Multan 66000, Pakistan*

Khamna Asad − *School of Biochemistry and Biotechnology, University of the Punjab, Lahore 54590, Pakistan*

Tehreem Ul Wara − *Department of Biochemistry, Bahauddin Zakariya University, Multan 66000, Pakistan*

Aqal Zaman − *Department of Microbiology & Molecular Genetics, Bahauddin Zakariya University, Multan 66000, Pakistan*

Riaz Ullah − *Department of Pharmacognosy, College of Pharmacy, King Saud University, Riyadh 11451, Saudi Arabia;* orcid.org/0000-0002-2860-467X

Essam A. Ali − *Department of Pharmaceutical Chemistry, College of Pharmacy, King Saud University, Riyadh 11451, Saudi Arabia*

Umar Nishan − *Department of Chemistry, Kohat University of Science & Technology, Kohat 26000, Pakistan;* orcid.org/0000-0002-0106-3068

Complete contact information is available at: https://pubs.acs.org/10.1021/acsomega.3c07866

Author Contributions

M.S., S.J. contributed equally to this work. Resource procurement, conceptualization, supervision, review and editing were done by M.S., E.A.A., and S.C.O. Formal analysis, investigation, writing the original draft were carried out by S.J., M.S., A.S., K.A., T.W., A.Z., and R.U. Visualization, review and editing were accomplished by R.U., E.A.A., and U.N. Funding acquisition was executed by E.A.A. S.C.O. All authors have read and agreed to the published version of the manuscript.

Funding

This research work was supported by the researchers supporting Project number (RSP-2023R45) King Saud University, Riyadh, Saudi Arabia. This work was also supported by the Doctoral Research Fund awarded to SCO.

Notes

The authors declare no competing financial interest.

■ ACKNOWLEDGMENTS

The authors wish to thank Researchers Supporting Project Number (RSP-2023R45) at King Saud University Riyadh, Saudi Arabia. We thank the Doctoral Research Fund, China, for financial support. The authors are also thankful to the Department of Biochemistry, Bahauddin Zakariya University, Multan, Pakistan, for providing the necessary infrastructure to perform this research.

■ REFERENCES

(1) Likos, A. M.; Sammons, S. A.; Olson, V. A.; Frace, A. M.; Li, Y.; Olsen-Rasmussen, M.; Davidson, W.; Galloway, R.; Khristova, M. L.; Reynolds, M. G.; Zhao, H.; Carroll, D. S.; Curns, A.; Formenty, P.; Esposito, J. J.; Regnery, R. L.; Damon, I. K. A Tale of Two Clades: Monkeypox Viruses. *J. Gen. Virol.* **2005**, *86* (10), 2661−2672.

(2) Howard, M.; Maki, J. J.; Connelly, S.; Hardy, D. J.; Cameron, A. Whole-Genome Sequences of Human Monkeypox Virus Strains from Two 2022 Global Outbreak Cases in Western New York State. *Microbiol. Resour. Announce.* **2022**, *11* (12), 20−23.

(3) Bahar, M. W.; Graham, S. C.; Chen, R. A. J.; Cooray, S.; Smith, G. L.; Stuart, D. I.; Grimes, J. M. How Vaccinia Virus Has Evolved to Subvert the Host Immune Response. *J. Struct. Biol.* **2011**, *175* (2), 127−134.

(4) Shchelkunov, S. N.; Totmenin, A. V.; Babkin, I. V.; Safronov, P. F.; Ryazankina, O. I.; Petrov, N. A.; Gutorov, V. V.; Uvarova, E. A.; Mikheev, M. V.; Sisler, J. R.; Esposito, J. J.; Jahrling, P. B.; Moss, B.; Sandakhchiev, L. S. Human Monkeypox and Smallpox Viruses: Genomic Comparison. *FEBS Lett.* **2001**, *509* (1), 66−70.

(5) Petersen, E.; Kantele, A.; Koopmans, M.; Asogun, D.; Yinka-Ogunleye, A.; Ihekweazu, C.; Zumla, A. Human Monkeypox: Epidemiologic and Clinical Characteristics, Diagnosis, and Prevention. *Infect. Dis. Clin. N. Am.* **2019**, *33* (4), 1027−1043.

(6) Ihekweazu, C.; Yinka-Ogunleye, A.; Lule, S.; Ibrahim, A. Importance of Epidemiological Research of Monkeypox: Is Incidence Increasing? *Expert Rev. Anti-Infect. Ther.* **2020**, *18* (5), 389−392.

(7) Fenner, F. Epidemiology and Evolution. *Medical Microbiology*; The University of Texas Medical Branch, 1996; pp 1−29.

(8) Magnus, P. v.; Andersen, E. K.; Petersen, K. B.; Birch-Andersen, A. A Pox-Like Disease in Cynomolgus Monkeys. *Acta Pathol. Microbiol. Scand.* **2009**, *46* (2), 156−176.

(9) McCollum, A. M.; Damon, I. K.; McCollum, A. M.; Damon, I. K. Human Monkeypox. *Clin. Infect. Dis.* **2014**, *58* (2), 260−267.

(10) Reed, K. D.; Melski, J. W.; Graham, M. B.; Regnery, R. L.; Sotir, M. J.; Wegner, M. V.; Kazmierczak, J. J.; Stratman, E. J.; Li, Y.; Fairley, J. A.; Swain, G. R.; Olson, V. A.; Sargent, E. K.; Kehl, S. C.; Frace, M. A.; Kline, R.; Foldy, S. L.; Davis, J. P.; Damon, I. K. The Detection of Monkeypox in Humans in the Western Hemisphere. *N. Engl. J. Med.* **2004**, *350* (4), 342−350.

(11) Zhang, Y.; Zhang, J.-Y.; Wang, F.-S. Monkeypox Outbreak: A Novel Threat after COVID-19? *Mil. Med. Res.* **2022**, *9* (1), 29.

(12) World Health Organization. *WHO Report: Holding Mass and Large Gathering Events during the Multi-Country Mpox Outbreak in the WHO European Region : Lessons Identified for Future Mass Gathering Preparedness*, 2023.

(13) Weinstein, R. A.; Nalca, A.; Rimoin, A. W.; Bavari, S.; Whitehouse, C. A. Reemergence of Monkeypox: Prevalence, Diagnostics, and Countermeasures. *Clin. Infect. Dis.* **2005**, *41* (12), 1765−1771.

(14) CDC Report. Treatment Information for Healthcare Professionals | Mpox | Poxvirus | CDC. https://www.cdc.gov/poxvirus/mpox/clinicians/treatment.html (accessed 2023-10-07).

(15) Rizk, J. G.; Lippi, G.; Henry, B. M.; Forthal, D. N.; Rizk, Y. Prevention and Treatment of Monkeypox. *Drugs* **2022**, *82* (9), 957−963.

(16) Shamim, M. A.; Padhi, B. K.; Satapathy, P.; Veeramachaneni, S. D.; Chatterjee, C.; Tripathy, S.; Akhtar, N.; Pradhan, A.; Dwivedi, P.; Mohanty, A.; Rodriguez-Morales, A. J.; Sah, R.; Al-Tammemi, A. B.; Al-Tawfiq, J. A.; Nowrouzi-Kia, B.; Chattu, V. K. The Use of Antivirals in the Treatment of Human Monkeypox Outbreaks: A Systematic Review. *Int. J. Infect. Dis.* **2023**, *127*, 150−161.

(17) Charles, I. K.; Iwunze, C. U.; Okeafor, B. M. K. Case Report: Deliberate Self-harm with Multiple Lacerations in a 23-year-old Depressed Nigerian Male Charles. *Port Harcourt Med. J.* **2018**, *11* (3), 170−174.

(18) Sah, R.; Paul, D.; Mohanty, A.; Shah, A.; Mohanasundaram, A. S.; Padhi, B. K. Monkeypox (Mpox) Vaccines and Their Side Effects: The Other Side of the Coin. *Int. J. Surg.* **2023**, *109* (2), 215−217.

(19) Sharff, K. A.; Tandy, T. K.; Lewis, P. F.; Johnson, E. S. *Cardiac Events Following JYNNEOS Vaccination for Prevention of Monkeypox*; Cold Spring Harbor Laboratory, 2022; pp 10−14.

(20) Zhang, C.; Maruggi, G.; Shan, H.; Li, J. Advances in MRNA Vaccines for Infectious Diseases. *Front. Immunol.* **2019**, *10* (MAR), 1−13.

(21) Al Fayez, N.; Nassar, M. S.; Alshehri, A. A.; Alnefaie, M. K.; Almughem, F. A.; Alshehri, B. Y.; Alawad, A. O.; Tawfik, E. A. Recent Advancement in MRNA Vaccine Development and Applications. *Pharmaceutics* **2023**, *15* (7), 1972.

(22) Sahin, U.; Karikó, K.; Türeci, Ö. MRNA-Based Therapeutics-Developing a New Class of Drugs. *Nat. Rev. Drug Discovery* **2014**, *13* (10), 759−780.

(23) Schlake, T.; Thess, A.; Fotin-Mleczek, M.; Kallen, K. J. Developing MRNA-Vaccine Technologies. *RNA Biol.* **2012**, *9* (11), 1319−1330.

(24) Xu, S.; Yang, K.; Li, R.; Zhang, L. mRNA Vaccine Era—Mechanisms, Drug Platform and Clinical Prospection. *Int. J. Mol. Sci.* **2020**, *21*, 6582.

(25) Ossato, A.; Tessari, R.; Trabucchi, C.; Zuppini, T.; Realdon, N.; Marchesini, F. Comparison of Medium-Term Adverse Reactions Induced by the First and Second Dose of MRNA BNT162b2 (Comirnaty, Pfizer-BioNTech) Vaccine: A Post-Marketing Italian Study Conducted between 1 January and 28 February 2021. *Eur. J. Hosp. Pharm.* **2023**, *30* (4), No. E15.

(26) Mulligan, M. J.; Lyke, K. E.; Kitchin, N.; Absalon, J.; Gurtman, A.; Lockhart, S.; Neuzil, K.; Raabe, V.; Bailey, R.; Swanson, K. A.; Li, P.; Koury, K.; Kalina, W.; Cooper, D.; Fontes-Garfias, C.; Shi, P. Y.; Türeci, Ö.; Tompkins, K. R.; Walsh, E. E.; Frenck, R.; Falsey, A. R.; Dormitzer, P. R.; Gruber, W. C.; Şahin, U.; Jansen, K. U. Phase I/II Study of COVID-19 RNA Vaccine BNT162b1 in Adults. *Nature* **2020**, *586* (7830), 589−593.

(27) Remichkova, M. Poxviruses: Smallpox Vaccine, Its Complications and Chemotherapy. *Virus Adapt. Treat.* **2010**, *2* (1), 41−46.

(28) Hall, T.; Biosciences, I.; Biosci, C. C.-G. B. BioEdit: An Important Software for Molecular Biology. *GERF Bull. Biosci.* **1991**, *2* (1), 60−61.

(29) Zhang, Q.; Wang, P.; Kim, Y.; Haste-Andersen, P.; Beaver, J.; Bourne, P. E.; Bui, H. H.; Buus, S.; Frankild, S.; Greenbaum, J.; Lund, O.; Lundegaard, C.; Nielsen, M.; Ponomarenko, J.; Sette, A.; Zhu, Z.; Peters, B. Immune Epitope Database Analysis Resource (IEDB-AR). *Nucleic Acids Res.* **2008**, *36*, 513−518.

(30) Jaan, S.; Zaman, A.; Ahmed, S.; Shah, M.; Ojha, S. C. MRNA Vaccine Designing Using Chikungunya Virus E Glycoprotein through Immunoinformatics-Guided Approaches. *Vaccines* **2022**, *10*, 1476.

(31) Aslam, M.; Shehroz, M.; Hizbullah; Shah, M.; Khan, M. A.; Afridi, S. G.; Khan, A. Potential Druggable Proteins and Chimeric Vaccine Construct Prioritization against Brucella Melitensis from Species Core Genome Data. *Genomics* **2020**, *112* (2), 1734−1745.

(32) Qasim, A.; Jaan, S.; Wara, T. U.; Shehroz, M.; Nishan, U.; Shams, S.; Shah, M.; Ojha, S. C. Computer-Aided Genomic Data Analysis of Drug-Resistant Neisseria Gonorrhoeae for the Identification of Alternative Therapeutic Targets. *Front. Cell. Infect. Microbiol.* **2023**, *13* (March), 1017315.

(33) Doytchinova, I. A.; Flower, D. R. VaxiJen: A Server for Prediction of Protective Antigens, Tumour Antigens and Subunit Vaccines. *BMC Bioinf.* **2007**, *8*, 4.

(34) Dimitrov, I.; Naneva, L.; Doytchinova, I.; Bangov, I. AllergenFP: Allergenicity Prediction by Descriptor Fingerprints. *Bioinformatics* **2014**, *30* (6), 846−851.

https://doi.org/10.1021/acsomega.3c07866
ACS Omega 2023, 8, 43341−43355

(35) Gupta, S.; Kapoor, P.; Chaudhary, K.; Gautam, A.; Kumar, R.; Raghava, G. P. S. In Silico Approach for Predicting Toxicity of Peptides and Proteins. *PLoS One* **2013**, *8* (9), No. e73957.
(36) Dhanda, S. K.; Vir, P.; Raghava, G. P. S. Designing of Interferon-Gamma Inducing MHC Class-II Binders. *Biol. Direct* **2013**, *8* (1), 30.
(37) Dhanda, S. K.; Gupta, S.; Vir, P.; Raghava, G. P. Prediction of IL4 Inducing Peptides. *Clin. Dev. Immunol.* **2013**, *2013*, 263952.
(38) Singh, O.; Hsu, W. L.; Su, E. C. Y. Ileukin10pred: A Computational Approach for Predicting Il-10-Inducing Immunosuppressive Peptides Using Combinations of Amino Acid Global Features. *Biology* **2021**, *11* (1), 5.
(39) Bhattacharya, M.; Malick, R. C.; Mondal, N.; Patra, P.; Pal, B. B.; Patra, B. C.; Kumar Das, B. Computational Characterization of Epitopic Region within the Outer Membrane Protein Candidate in Flavobacterium Columnare for Vaccine Development. *J. Biomol. Struct. Dyn.* **2020**, *38* (2), 450−459.
(40) Aslam, M.; Shehroz, M.; Ali, F.; Zia, A.; Pervaiz, S.; Shah, M.; Hussain, Z.; Nishan, U.; Zaman, A.; Afridi, S. G.; Khan, A. Chlamydia Trachomatis Core Genome Data Mining for Promising Novel Drug Targets and Chimeric Vaccine Candidates Identification. *Comput. Biol. Med.* **2021**, *136* (July), 104701.
(41) Vita, R.; Mahajan, S.; Overton, J. A.; Dhanda, S. K.; Martini, S.; Cantrell, J. R.; Wheeler, D. K.; Sette, A.; Peters, B. The Immune Epitope Database (IEDB): 2018 Update. *Nucleic Acids Res.* **2019**, *47* (D1), D339−D343.
(42) Jaan, S.; Shah, M.; Ullah, N.; Amjad, A.; Javed, M. S.; Nishan, U.; Mustafa, G.; Nawaz, H.; Ahmed, S.; Ojha, S. C. Multi-Epitope Chimeric Vaccine Designing and Novel Drug Targets Prioritization against Multi-Drug Resistant Staphylococcus Pseudintermedius. *Front. Microbiol.* **2022**, *13* (August), 1−19.
(43) Cash, P. 2-D Proteome Analysis Protocols. *Cell Biol. Int.* **1999**, *23* (5), 385.
(44) Magnan, C. N.; Randall, A.; Baldi, P. SOLpro: Accurate Sequence-Based Prediction of Protein Solubility. *Bioinformatics* **2009**, *25* (17), 2200−2207.
(45) Geourjon, C.; Deléage, G. Sopma: Significant Improvements in Protein Secondary Structure Prediction by Consensus Prediction from Multiple Alignments. *Bioinformatics* **1995**, *11* (6), 681−684.
(46) Waterhouse, A.; Bertoni, M.; Bienert, S.; Studer, G.; Tauriello, G.; Gumienny, R.; Heer, F. T.; de Beer, T. A.; Rempfer, C.; Bordoli, L.; Lepore, R.; Schwede, T. SWISS-MODEL: Homology Modelling of Protein Structures and Complexes. *Nucleic Acids Res.* **2018**, *46* (W1), W296−W303.
(47) Heo, L.; Park, H.; Seok, C. GalaxyRefine: Protein Structure Refinement Driven by Side-Chain Repacking. *Nucleic Acids Res.* **2013**, *41* (W1), 384−388.
(48) Laskowski, R. A.; MacArthur, M. W.; Moss, D. S.; Thornton, J. M. PROCHECK: A Program to Check the Stereochemical Quality of Protein Structures. *J. Appl. Crystallogr.* **1993**, *26* (2), 283−291.
(49) Shah, M.; Anwar, A.; Qasim, A.; Jaan, S.; Sarfraz, A.; Ullah, R.; Ali, E. A.; Nishan, U.; Shehroz, M.; Zaman, A.; Ojha, S. C. Proteome Level Analysis of Drug-Resistant Prevotella Melaninogenica for the Identification of Novel Therapeutic Candidates. *Front. Microbiol.* **2023**, *14*, 1271798.
(50) Ponomarenko, J.; Bui, H. H.; Li, W.; Fusseder, N.; Bourne, P. E.; Sette, A.; Peters, B. ElliPro: A New Structure-Based Tool for the Prediction of Antibody Epitopes. *BMC Bioinf.* **2008**, *9*, 514.
(51) Vilar, S.; Cozza, G.; Moro, S. Medicinal Chemistry and the Molecular Operating Environment (MOE): Application of QSAR and Molecular Docking to Drug Discovery. *Curr. Top. Med. Chem.* **2008**, *8* (18), 1555−1572.
(52) Qureshi, N. A.; Bakhtiar, S. M.; Faheem, M.; Shah, M.; Bari, A.; Mahmood, H. M.; Sohaib, M.; Mothana, R. A.; Ullah, R.; Jamal, S. B. Genome-Based Drug Target Identification in Human Pathogen Streptococcus Gallolyticus. *Front. Genet.* **2021**, *12* (March), 1−20.
(53) Kozakov, D.; Hall, D. R.; Xia, B.; Porter, K. A.; Padhorny, D.; Yueh, C.; Beglov, D.; Vajda, S. The ClusPro Web Server for Protein-Protein Docking. *Nat. Protoc.* **2017**, *12* (2), 255−278.
(54) López-Blanco, J. R.; Aliaga, J. I.; Quintana-Ortí, E. S.; Chacón, P. IMODS: Internal Coordinates Normal Mode Analysis Server. *Nucleic Acids Res.* **2014**, *42* (W1), 271−276.
(55) Bowers, K. J.; Chow, E.; Xu, H.; Dror, R. O.; Eastwood, M. P.; Gregersen, B. A.; Klepeis, J. L.; Kolossvary, I.; Moraes, M. A.; Sacerdoti, F. D.; Salmon, J. K.; Shan, Y.; Shaw, D. E. Scalable Algorithms for Molecular Dynamics Simulations on Commodity Clusters. In *Proceedings of the 2006 ACM/IEEE Conference on Supercomputing*; IEEE, 2006; p 43.
(56) Hildebrand, P. W.; Rose, A. S.; Tiemann, J. K. S. Bringing Molecular Dynamics Simulation Data into View. *Trends Biochem. Sci.* **2019**, *44* (11), 902−913.
(57) Madhavi Sastry, G.; Adzhigirey, M.; Day, T.; Annabhimoju, R.; Sherman, W. Protein and Ligand Preparation: Parameters, Protocols, and Influence on Virtual Screening Enrichments. *J. Comput.-Aided Mol. Des.* **2013**, *27* (3), 221−234.
(58) Shivakumar, D.; Williams, J.; Wu, Y.; Damm, W.; Shelley, J.; Sherman, W. Prediction of Absolute Solvation Free Energies Using Molecular Dynamics Free Energy Perturbation and the OPLS Force Field. *J. Chem. Theory Comput.* **2010**, *6* (5), 1509−1519.
(59) Castiglione, F.; Bernaschi, M. C-Immsim: Playing with the Immune Response. *Proceedings of the Sixteenth International Symposium on Mathematical Theory of Networks and Systems (MTNS2004)*, 2004; pp 1−7.
(60) Almofti, Y. A.; Abd-elrahman, K. A.; Eltilib, E. E. M. Vaccinomic Approach for Novel Multi Epitopes Vaccine against Severe Acute Respiratory Syndrome Coronavirus-2 (SARS-CoV-2). *BMC Immunol.* **2021**, *22* (1), 22.
(61) Grote, A.; Hiller, K.; Scheer, M.; Munch, R.; Nortemann, B.; Hempel, D. C.; Jahn, D. JCat: A Novel Tool to Adapt Codon Usage of a Target Gene to Its Potential Expression Host. *Nucleic Acids Res.* **2005**, *33*, 526−531.
(62) Stenström, C.; Holmgren, E.; Isaksson, L. A. Cooperative Effects by the Initiation Codon and Its Flanking Regions on Translation Initiation. *Gene* **2001**, *273* (2), 259−265.
(63) Ahammad, I.; Lira, S. S. Designing a novel mRNA vaccine against SARS-CoV-2: An immunoinformatics approach. *Int. J. Biol. Macromol.* **2020**, *162*, 820−837.
(64) Zuker, M. Mfold Web Server for Nucleic Acid Folding and Hybridization Prediction. *Nucleic Acids Res.* **2003**, *31* (13), 3406−3415.
(65) Grote, A.; Hiller, K.; Scheer, M.; Munch, R.; Nortemann, B.; Hempel, D. C.; Jahn, D. JCat: A Novel Tool to Adapt Codon Usage of a Target Gene to Its Potential Expression Host. *Nucleic Acids Res.* **2005**, *33* (Suppl. 2), 526−531.
(66) Dey, J.; Mahapatra, S. R.; Patnaik, S.; Lata, S.; Kushwaha, G. S.; Panda, R. K.; Misra, N.; Suar, M. Molecular Characterization and Designing of a Novel Multiepitope Vaccine Construct Against Pseudomonas Aeruginosa. *Int. J. Pept. Res. Ther.* **2022**, *28* (2), 49.
(67) Kaushik, V.; Jain, P.; Akhtar, N.; Joshi, A.; Gupta, L. R.; Grewal, R. K.; Oliva, R.; Shaikh, A. R.; Cavallo, L.; Chawla, M. Immunoinformatics-Aided Design and *In Vivo* Validation of a Peptide-Based Multiepitope Vaccine Targeting Canine Circovirus. *ACS Pharmacol. Transl. Sci.* **2022**, *5* (8), 679−691.
(68) Akhtar, N.; Kaushik, V.; Grewal, R. K.; Wani, A. K.; Suwattanasophon, C.; Choowongkomon, K.; Oliva, R.; Shaikh, A. R.; Cavallo, L.; Chawla, M. Immunoinformatics-Aided Design of a Peptide Based Multiepitope Vaccine Targeting Glycoproteins and Membrane Proteins against Monkeypox Virus. *Viruses* **2022**, *14* (11), 2374.
(69) Akhtar, N.; Magdaleno, J. S. L.; Ranjan, S.; Wani, A. K.; Grewal, R. K.; Oliva, R.; Shaikh, A. R.; Cavallo, L.; Chawla, M. Secreted Aspartyl Proteinases Targeted Multi-Epitope Vaccine Design for Candida Dubliniensis Using Immunoinformatics. *Vaccines* **2023**, *11* (2), 364.
(70) Kaushik, V.; G, S. K.; Gupta, L. R.; Kalra, U.; Shaikh, A. R.; Cavallo, L.; Chawla, M. Immunoinformatics Aided Design and In-Vivo Validation of a Cross-Reactive Peptide Based Multi-Epitope

https://doi.org/10.1021/acsomega.3c07866
ACS Omega 2023, 8, 43341−43355

Vaccine Targeting Multiple Serotypes of Dengue Virus. *Front. Immunol.* **2022**, *13*, 865180.
(71) Philpott, D.; Hughes, C. M.; Alroy, K. A.; Kerins, J. L.; Pavlick, J.; Asbel, L.; Crawley, A.; Newman, A. P.; Spencer, H.; Feldpausch, A.; et al. Epidemiologic and Clinical Characteristics of Monkeypox Cases — United States, May 17−July 22, 2022. *MMWR-Morbidity and Mortality Weekly Report* **2022**, *71* (32), 1018−1022.
(72) Durski, K. N.; McCollum, A. M.; Nakazawa, Y.; Petersen, B. W.; Reynolds, M. G.; Briand, S.; Djingarey, M. H.; Olson, V.; Damon, I. K.; Khalakdina, A. Emergence of Monkeypox—West and Central Africa, 1970−2017 (Vol 67, Pg 306, 2018). *MMWR-Morbidity and Mortality Weekly Report* **2018**, *67* (16), 479.
(73) Fine, P. E.; Jezek, Z.; Grab, B.; Dixon, H. The transmission potential of monkeypox virus in human populations. *Int. J. Epidemiol.* **1988**, *17* (3), 643−650.
(74) Huang, T.; Peng, L.; Han, Y.; Wang, D.; He, X.; Wang, J.; Ou, C. Lipid Nanoparticle-Based MRNA Vaccines in Cancers: Current Advances and Future Prospects. *Front. Immunol.* **2022**, *13*, 922301.
(75) Liang, Y.; Huang, L.; Liu, T. Development and Delivery Systems of MRNA Vaccines. *Front. Bioeng. Biotechnol.* **2021**, *9*, 718753.
(76) Schnee, M.; Vogel, A. B.; Voss, D.; Petsch, B.; Baumhof, P.; Kramps, T.; Stitz, L. An MRNA Vaccine Encoding Rabies Virus Glycoprotein Induces Protection against Lethal Infection in Mice and Correlates of Protection in Adult and Newborn Pigs. *PLoS Neglected Trop. Dis.* **2016**, *10* (6), No. e0004746.
(77) Al Fayez, N.; Nassar, M. S.; Alshehri, A. A.; Alnefaie, M. K.; Almughem, F. A.; Alshehri, B. Y.; Alawad, A. O.; Tawfik, E. A. Recent Advancement in MRNA Vaccine Development and Applications. *Pharmaceutics* **2023**, *15* (7), 1972.
(78) Chen, P.; Shi, X.; He, W.; Zhong, G.; Tang, Y.; Wang, H.; Zhang, P. MRNA Vaccine-a Desirable Therapeutic Strategy for Surmounting COVID-19 Pandemic. *Hum. Vaccines Immunother.* **2022**, *18* (1), 1−13.
(79) Le, T. K.; Paris, C.; Khan, K. S.; Robson, F.; Ng, W. L.; Rocchi, P. Nucleic Acid-Based Technologies Targeting Coronaviruses. *Trends Biochem. Sci.* **2021**, *46* (5), 351−365.
(80) Ljunggren, G.; Anderson, D. J. Cytokine Induced Modulation of MHC Class I and Class II Molecules on Human Cervical Epithelial Cells. *J. Reprod. Immunol.* **1998**, *38* (2), 123−138.
(81) Parvizpour, S.; Pourseif, M. M.; Razmara, J.; Rafi, M. A.; Omidi, Y. Epitope-Based Vaccine Design: A Comprehensive Overview of Bioinformatics Approaches. *Drug Discovery Today* **2020**, *25* (6), 1034−1042.
(82) Suleman, M.; Rashid, F.; Ali, S.; Sher, H.; Luo, S.; Xie, L.; Xie, Z. Immunoinformatic-Based Design of Immune-Boosting Multi-epitope Subunit Vaccines against Monkeypox Virus and Validation through Molecular Dynamics and Immune Simulation. *Front. Immunol.* **2022**, *13*, 1042997.
(83) Khan, A.; Khan, S.; Saleem, S.; Nizam-Uddin, N.; Mohammad, A.; Khan, T.; Ahmad, S.; Arshad, M.; Ali, S. S.; Suleman, M.; Wei, D.-Q. Immunogenomics Guided Design of Immunomodulatory Multi-Epitope Subunit Vaccine against the SARS-CoV-2 New Variants, and Its Validation through in Silico Cloning and Immune Simulation. *Comput. Biol. Med.* **2021**, *133*, 104420.
(84) Sami, S. A.; Marma, K. K. S.; Mahmud, S.; Khan, M. A. N.; Albogami, S.; El-Shehawi, A. M.; Rakib, A.; Chakraborty, A.; Mohiuddin, M.; Dhama, K.; Uddin, M. M. N.; Hossain, M. K.; Tallei, T. E.; Emran, T. B.. Designing of a Multi-Epitope Vaccine against the Structural Proteins of Marburg Virus Exploiting the Immunoinformatics Approach. *ACS Omega* **2021**, *6* (47), 32043−32071.
(85) Shah, S. Z.; Jabbar, B.; Mirza, M. U.; Waqas, M.; Aziz, S.; Halim, S. A.; Ali, A.; Rafique, S.; Idrees, M.; Khalid, A.; Abdalla, A. N.; Khan, A.; Al-Harrasi, A. An Immunoinformatics Approach to Design a Potent Multi-Epitope Vaccine against Asia-1 Genotype of Crimean-Congo Haemorrhagic Fever Virus Using the Structural Glycoproteins as a Target. *Vaccines* **2022**, *11* (1), 61.
(86) Touhidinia, M.; Sefid, F.; Bidakhavidi, M. Design of a Multi-Epitope Vaccine Against Acinetobacter Baumannii Using Immunoinformatics Approach. *Int. J. Pept. Res. Ther.* **2021**, *27* (4), 2417−2437.
(87) Jalal, K.; Abu-Izneid, T.; Khan, K.; Abbas, M.; Hayat, A.; Bawazeer, S.; Uddin, R. Identification of Vaccine and Drug Targets in Shigella Dysenteriae Sd197 Using Reverse Vaccinology Approach. *Sci. Rep.* **2022**, *12* (1), 251.
(88) Kou, Y.; Xu, Y.; Zhao, Z.; Liu, J.; Wu, Y.; You, Q.; Wang, L.; Gao, F.; Cai, L.; Jiang, C. Tissue Plasminogen Activator (TPA) Signal Sequence Enhances Immunogenicity of MVA-Based Vaccine against Tuberculosis. *Immunol. Lett.* **2017**, *190*, 51−57.
(89) Fadaka, A. O.; Sibuyi, N. R. S.; Martin, D. R.; Goboza, M.; Klein, A.; Madiehe, A. M.; Meyer, M. Immunoinformatics Design of a Novel Epitope-Based Vaccine Candidate against Dengue Virus. *Sci. Rep.* **2021**, *11* (1), 19707.
(90) Aziz, S.; Almajhdi, F. N.; Waqas, M.; Ullah, I.; Salim, M. A.; Khan, N. A.; Ali, A. Contriving Multi-Epitope Vaccine Ensemble for Monkeypox Disease Using an Immunoinformatics Approach. *Front. Immunol.* **2022**, *13* (October), 1−24.
(91) Waqas, M.; Aziz, S.; Liò, P.; Khan, Y.; Ali, A.; Iqbal, A.; Khan, F.; Almajhdi, F. N. Immunoinformatics Design of Multivalent Epitope Vaccine against Monkeypox Virus and Its Variants Using Membrane-Bound, Enveloped, and Extracellular Proteins as Targets. *Front. Immunol.* **2023**, *14* (January), 1−21.

https://doi.org/10.1021/acsomega.3c07866
ACS Omega 2023, 8, 43341−43355